

**Dynamic sea level
rise pattern from
land-ice**

T. Howard et al.

This discussion paper is/has been under review for the journal Ocean Science (OS).
Please refer to the corresponding final paper in OS if available.

The land-ice contribution to 21st century dynamic sea-level rise

**T. Howard¹, J. Ridley¹, A. K. Pardaens¹, R. T. W. L. Hurkmans², A. J. Payne²,
R. H. Giesen³, J. A. Lowe¹, J. L. Bamber², T. L. Edwards², and J. Oerlemans³**

¹Met Office Hadley Centre, FitzRoy Road, Exeter, EX1 3PB, UK

²Bristol Glaciology Centre, School of Geographical Sciences,
University of Bristol, University Road, Bristol, BS8 1SS, UK

³Institute for Marine and Atmospheric research Utrecht, Utrecht University, P.O. Box 80005,
3508 TA Utrecht, the Netherlands

Received: 6 December 2013 – Accepted: 12 December 2013 – Published: 13 January 2014

Correspondence to: T. Howard (tom.howard@metoffice.gov.uk)
and J. Ridley (jeff.rodley@metoffice.gov.uk)

Published by Copernicus Publications on behalf of the European Geosciences Union.

Title Page

Abstract

Introduction

Conclusions

References

Tables

Figures

⏪

⏩

◀

▶

Back

Close

Full Screen / Esc

Printer-friendly Version

Interactive Discussion



Abstract

Climate change has the potential to locally influence mean sea level through a number of processes including (but not limited to) thermal expansion of the oceans and enhanced land ice melt. These lead to departures from the global mean sea level change, due to spatial variations in the change of water density and transport, which are termed dynamic sea level changes.

In this study we present regional patterns of sea-level change projected by a global coupled atmosphere–ocean climate model forced by projected ice-melt fluxes from three sources: the Antarctic ice sheet, the Greenland ice sheet and small glaciers and ice caps. The largest ice melt flux we consider is equivalent to almost 0.7 m of global sea level rise over the 21st century. Since the ice melt is not constant, the evolution of the dynamic sea level changes is analysed.

We find that the dynamic sea level change associated with the ice melt is small, with the largest changes, occurring in the North Atlantic, contributing of order 3 cm above the global mean rise. Furthermore, the dynamic sea level change associated with the ice melt is similar regardless of whether the simulated ice fluxes are applied to a simulation with fixed or changing atmospheric CO₂.

1 Introduction

Sea-level rise has the potential to lead to substantial impacts on society and ecosystems (Nicholls et al., 2011). Global mean sea-level rise (SLR) is comprised of thermal expansion, additional melt water from changes in land-based-ice mass balance, and other changes in terrestrial water storage (Church et al., 2011). Projected time-mean SLR for a particular location consists of a component from the global mean change, together with a component from changes in the spatial variation of sea level relative to the global mean (e.g. Milne et al., 2009). This change in spatial variation is potentially influenced by the interplay of changes in ocean dynamics and spatial variations in

OSD

11, 123–169, 2014

Dynamic sea level rise pattern from land-ice

T. Howard et al.

Title Page

Abstract

Introduction

Conclusions

References

Tables

Figures

◀

▶

◀

▶

Back

Close

Full Screen / Esc

Printer-friendly Version

Interactive Discussion



Dynamic sea level rise pattern from land-ice

T. Howard et al.

Title Page

Abstract

Introduction

Conclusions

References

Tables

Figures

◀

▶

◀

▶

Back

Close

Full Screen / Esc

Printer-friendly Version

Interactive Discussion



density of the water column. In addition, a change in the mass load of the land-based ice affects the sea level pattern through changes to the gravity field and through the vertical land movement response (giving sea level “fingerprints” of these changes in ice mass). Regional variations in vertical land-movement, from responses to both projected and paleo changes in ice load, and from factors such as tectonic movement or ground water extraction, play a role in the amount of SLR experienced at a particular location (relative SLR).

The largest uncertainty in projections of SLR to date is in the contribution from land-based ice melt, in particular related to the enhanced ice sheet dynamics arising from ocean-ice sheet interactions (Prichard et al., 2009). Climate change could trigger an increase in the ice-dynamical flow either from the formation of melt ponds on the upper surface of ice shelves (Bevan et al., 2012; McGrath et al., 2012), which may destabilize them, or by increases in submarine melt experienced by ice shelves (Prichard et al., 2012) and marine-terminating glaciers (Meier and Post, 1987; Barrand et al., 2013) as a consequence of oceanic warming, which leads to their thinning (Stanton et al., 2013).

A basic approach to estimating the contribution of the ice sheets to SLR, is a qualitative analysis of the physically tenable accelerated ice discharge (Pfeffer et al., 2008), which suggests a “most likely” 21st-century SLR of 0.8 m. However, the intermittent nature of ice-sheet glacial discharge would point to a lower potential contribution from Greenland (Van den Broeke et al., 2011). Pfeffer et al. (2008) also considered whether a total SLR of 2 m to 2100 was physically tenable and concluded that while it could potentially occur, it would need upper limits of plausible glaciological behaviour. Recent years have also seen a further focus on improved sensitivity studies. The SeaRise program estimated the upper bound of ice sheet contributions to sea level over the next 100–200 yr, through a set of commonly forced ice sheet models (Bindschadler et al., 2013; Nowicki et al., 2013a, b). The Ice2sea program focused on reducing uncertainty of the future contribution of ice sheets to SLR, through observations and improved ice sheet models (Gillet-Chaulet et al., 2012; Timmermann et al., 2012; Nick et al., 2013; Pattyn et al., 2012; Seddik et al., 2012). Seddik et al. (2012) using a full Stokes model

(and a shallow ice model) project a Greenland contribution to sea-level rise of order 12 cm (15 cm) over the next 100 yr under a scenario with combined global warming and doubled basal sliding.

Physically-based process models have been used to assess the future SLR impact of fast flowing glaciers and ice shelf basal melt. The mass loss associated with the atmosphere and ocean interaction with the glaciers fringing the Greenland ice sheet can be approximated through flow-line models of the major outlet glaciers (Nick et al., 2013), or included in ice sheet models either as parameterisations of the flow-line models (Goelzer et al., 2013) or by enhanced basal sliding (Graversen et al., 2011) to capture the effect of increased outflow.

Projected changes in the patterns of dynamic sea-level (DSL), where this term is used here to denote the pattern of regional sea level change relative to the global mean, which is related to the ocean circulation, have been investigated in a number of previous studies. DSL is projected to change under the influence of greenhouse gas warming (e.g. Meehl et al., 2007; Lowe and Gregory, 2006). There is, however, considerable uncertainty in the pattern of SLR given by different models for projections under a common scenario, with differing patterns and/or magnitudes of regional deviations (e.g. Gregory et al., 2005; Meehl et al., 2007; Paradaens et al., 2011). DSL is also affected in sensitivity studies which apply an increase in surface freshwater input to the northern Atlantic (e.g. Stouffer et al., 2006), in some cases with this additional water confined around Greenland to represent additional ice sheet melt, (e.g. Swingedouw et al., 2013). A common feature of the projected patterns of sea level change is a notable increase in DSL in the North Atlantic (Yin et al., 2009; Yin, 2012).

Many of the Atlantic features of sea-level pattern change in these experiments have been related to induced changes in the Meridional Overturning Circulation (MOC), for example a dipole or tripole pattern of change in spatial variations in the North Atlantic (e.g. Levermann et al., 2005; Meehl et al., 2007; Lorbacher et al., 2010). The weakening of the MOC, as predicted by climate models, is generally understood to be the result of increased buoyancy input to the North Atlantic in a warmer climate (Schmittner et al.,

Dynamic sea level rise pattern from land-ice

T. Howard et al.

Title Page

Abstract

Introduction

Conclusions

References

Tables

Figures



Back

Close

Full Screen / Esc

Printer-friendly Version

Interactive Discussion



**Dynamic sea level
rise pattern from
land-ice**

T. Howard et al.

Title Page

Abstract

Introduction

Conclusions

References

Tables

Figures

◀

▶

◀

▶

Back

Close

Full Screen / Esc

Printer-friendly Version

Interactive Discussion



2005; Meehl et al., 2007). The effect of surface heat flux changes rather than surface
freshwater flux changes has generally been found to dominate the MOC response in
greenhouse gas warming simulations (e.g. Gregory et al., 2005), but increased fresh-
water flux to the northern Atlantic has also been found to have an important effect (e.g.
5 Stouffer et al., 2007). Widely different sensitivities of the MOC, either to a common
greenhouse gas warming scenario (e.g. Meehl et al., 2007) or to an additional north-
ern Atlantic water flux under a common experimental design (e.g. Stouffer et al., 2006),
have been found. The effects of scenarios of additional Greenland melt water on north-
ern Atlantic regional sea level, from the effects of DSL change together with ice mass
10 change fingerprints indicate that the fingerprint from MOC slowing is dependent on the
ice melt geometry (Kopp et al., 2010).

A number of model studies have made projections of greater complexity, with
a Greenland ice sheet model embedded in a coupled climate model. These more inter-
active studies have differed in the degree to which they have found additional meltwater
15 to slow the MOC. Ridley et al. (2005), for example, find a small reduction of 1–2 Sver-
drups (one Sverdrup is $10^6 \text{ m}^3 \text{ s}^{-1}$, henceforth Sv) in the MOC under a $4 \times \text{CO}_2$ forcing
experiment with the HadCM3 model, where the maximum freshwater flux from Green-
land melt reached 0.06 Sv. In contrast, Mikolajewicz et al. (2007) found no influence
of up to 0.1 Sv of Greenland melt-water on the MOC. The ice sheet models in these
20 linked climate-ice-sheet model simulations do not include processes such as accel-
erated ice sheet dynamics; however the more idealised sensitivity study scenarios of
additional freshwater input provide information on the potential impacts of such higher
melt scenarios.

The input, into an ocean-ice model, of idealised freshwater fluxes from ice melt
25 can lead to a rapid (days) barotropic adjustment of the sea level pattern in a non-
Boussinesq model (Lorbacher et al., 2012). In a Boussinesq model it takes decades
for the diagnosed DSL to equilibrate, after input of Greenland melt-water, across the
globe (Wang et al., 2012). In the latter model the main DSL change remains in the

North Atlantic. The idealised freshwater fluxes above are sufficiently large to attribute all change to the ice sheet component of sea level rise, rather than internal variability.

In this study we give projections of DSL change associated with new case study scenarios of land-based ice melt. We use a small ensemble of simulations to determine the detectability of DSL changes from relatively small freshwater fluxes. We consider the role of this additional freshwater input to the ocean both for pre-industrial radiative forcing conditions and under the SRES A1B greenhouse gas warming scenario, which is usually regarded as a medium business-as-usual (BAU) emissions scenario. We include two ice melt scenarios which are provided by the European Union Ice2Sea project, and which include updated projections of the Glacier and Ice Cap (G&IC) contribution and Greenland and Antarctic ice sheet freshwater contributions. The ice sheet components are derived from simplified simulations which include information about likely regions of dynamical instability.

2 Case study scenarios of ice-melt freshwater flux

Two plausible scenarios of future freshwater flux, from Glaciers and Ice Caps (G&IC), and the Greenland and Antarctic ice sheets, were developed. The freshwater fluxes were based on modelling of the respective ice masses, and are termed the mid-range (MR) and high-end (HE) scenarios. The ice mass changes are converted to equivalent freshwater fluxes (Fig. 1 shows the globally-integrated values) and applied to the HadCM3 model ocean as anomalies relative to appropriate reference periods (during which the particular component was assumed to be in steady state). The freshwater fluxes are applied to one of 28 ocean sectors (16 for G&IC, 5 for Greenland and 7 for Antarctica) which are defined within HadCM3 (Fig. 2). Melt water is allocated to the nearest coastal sector and the freshwater flux applied equally to all gridcells along that sector. Figure 2 shows the ocean grid points involved in the freshwater forcing, coloured by the tercile of freshwater flux integrated over the full 150 yr period of simulation. The

Dynamic sea level rise pattern from land-ice

T. Howard et al.

Title Page

Abstract

Introduction

Conclusions

References

Tables

Figures



Back

Close

Full Screen / Esc

Printer-friendly Version

Interactive Discussion



projected freshwater fluxes were derived from models which used forcing fields from the ECHAM5 coupled climate model, under an SRES A1B scenario.

The key sources of uncertainty are the future scenario (SRES A1B) and the scaling of the ice response to represent high and midrange outcomes. For example the G&IC melt rates are scaled versions of present day temperature sensitivities, which may not be applicable late in the 21st C because some glaciers will be depleted. The ice sheet dynamic response is scaled to “high end” freshwater fluxes by increasing the basal lubrication of the outlet glaciers. This may not be an appropriate solution as the ice sheet basal sliding may not scale linearly in the future.

2.1 Glaciers and Ice Caps melt water component

The G&IC component of ice mass change was derived from a regionalized glacier mass balance model that uses projected temperature and precipitation anomalies for 19 glacierized sectors (Giesen and Oerlemans, 2012). In this model, sensitivities of the regional G&IC responses were calibrated using automatic weather station data for 80 benchmark glaciers. A calibrated version of the projected volume changes (1980–2100) was used for the MR scenario and the HE scenario was obtained by simply perturbing the melt parameters to the high plausible limit. Only the equivalent positive fluxes of net-melt-water were transferred to the ocean and assumed, as an approximation, to be solely due to an increase in melt-runoff rather than from any reduction in accumulation. An approximate G&IC steady state (with zero flux anomalies) was assumed for 1860, with the calculated fluxes interpolated back to this point. Fluxes from the peripheral G&IC around the ice sheets, not directly attached to the ice sheet, were assigned to the G&IC water flux.

The total sea level equivalent (SLE) of the G&IC freshwater fluxes, for the 2090–2099 period relative to the 1980–1999 period is 0.13 m and 0.22 m for the MR and HE scenarios, respectively. These estimates are in good agreement with others. Projections for the G&IC component of sea-level rise from the 5th Coupled Model Intercomparison Project (CMIP5), relative to the 1986–2005 mean at 2100, are: 0.17 m (RCP4.5)

Dynamic sea level rise pattern from land-ice

T. Howard et al.

Title Page

Abstract

Introduction

Conclusions

References

Tables

Figures



Back

Close

Full Screen / Esc

Printer-friendly Version

Interactive Discussion



identifies a range of 4 to 12 mm, while Graversen et al. (2011) and Furst et al. (2013) identify higher-end values of 16 and 45 mm, respectively. However, these models do not explicitly address the issue of the fast flowing tide-water glaciers simulated by Nick et al. (2013) where the fast dynamical component is estimated to be (referenced to the 1986–2005 mean) 85 mm for RCP8.5 and 63 mm for RCP4.5 by 2100. Thus, as a whole there is considerable uncertainty for the future dynamical changes to the ice sheet, but our own estimates are arguably at the low end for the mid-range scenario.

For Greenland, the overall SLE (calving and runoff) for our MR and HE scenarios is 0.04 m and 0.08 m by 2100, while the AR5 medians are 0.08 m for RCP4.5 to 0.12 m for RCP8.5.

2.3 Antarctic ice sheet component of freshwater

For the Antarctic ice sheet, freshwater fluxes into the ocean are assumed to come from iceberg calving and the marine melt of ice shelves alone (surface runoff being negligible). These fluxes are derived from the simulations of Ritz et al. (2013) in which grounding line retreat scenarios are imposed on the modelled ice sheet. The simulations include the ice shelf basal melt, leading to rapid ice dynamics, and grounding line retreat, which leads to marine ice sheet instability (Binschadler, 2006). The resulting 1000 model ensemble has individual members weighted according to their success in simulating present-day sea level contribution. The HE estimate is that of a single member of the ensemble that lies close to the 99.9 % probability threshold for ice mass loss, while the MR estimate is a single member closest to the maximum likelihood at 2100. The HE SLR between 2006 and 2100 is 311 mm and the MR SLR 99 mm.

The freshwater fluxes were allocated to 15 ice sheet drainage basins and uniformly distributed along adjacent HadCM3 coastal sector grid cells. In accordance with observations (Pritchard et al., 2012) most of the melt occurs in the Amundsen Sea (west of the Antarctic Peninsula). A steady state is again assumed in 1992, as this was when the first evidence of instabilities in the ice sheet was suggested (Doake and Vaughan, 1991; Jacobs et al., 1992), with the freshwater fluxes interpolated back to zero anomalies at

Dynamic sea level rise pattern from land-ice

T. Howard et al.

Title Page

Abstract

Introduction

Conclusions

References

Tables

Figures

◀

▶

◀

▶

Back

Close

Full Screen / Esc

Printer-friendly Version

Interactive Discussion



this time. For comparison, the SLE (including changes in accumulation and marine melt/calving, but not marine ice sheet instability) for CMIP5 are 0.05 m (RCP4.5) and 0.04 m (RCP8.5), respectively.

2.4 Processing of freshwater fluxes

5 An 11 yr smoothing was applied to the freshwater fluxes. In Antarctica, this is justified because the icebergs take several years to melt, which would act as a natural smoothing function. In Greenland, it may be justified because the iceberg discharge may not be synchronous along each coastline sector. The smoothed fluxes retain significant variability over timescales of a few years (Fig. 1a). This is particularly the case
10 for the HE Greenland and Antarctic scenarios. For Greenland, the transient pulses of water are from enhanced calving, which originates from the flow line simulations of Helheim glacier, which was upscaled to the rest of the south-east Greenland sector (Nick et al., 2013). The pulse originates from a temporary instability associated with an unusually warm local ocean temperature, which is in line with evidence of an ocean-
15 forced synchronised glacier acceleration in SE Greenland (Christoffersen et al., 2011) and SW Greenland (Holland et al., 2008) in the early 2000s. The simplified simulations used here may, however, overemphasize the degree of synchronicity. In Antarctica, the transient pulses arise from marine ice sheet instability, with the rapid retreat of the grounding line resulting in large losses of ice. The first peak is associated with a partial
20 collapse of the west Antarctic ice sheet in the region of Pine Island, as predicted (Cornford et al., 2013). The final peak occurs with another partial collapse of the west Antarctic ice sheet in the region of the Filchner Ice Shelf as depicted in some simulations (Hellmer et al., 2012).

25 The total SLE for the MR and HE scenarios for 2090–2099 (referenced to 1860–1870) is 0.26 and 0.57 m, respectively, while from AR5 the mean SLR given from all land-based ice masses is 0.25 m (RCP4.5) and 0.32 m (RCP8.5) – estimates which include the ice sheet rapid dynamics, but not the marine ice sheet instability (which dominates the SLE at 2100 for the HE scenario).

Dynamic sea level rise pattern from land-ice

T. Howard et al.

Title Page

Abstract

Introduction

Conclusions

References

Tables

Figures



Back

Close

Full Screen / Esc

Printer-friendly Version

Interactive Discussion



3 Model formulation

The simulations used in this study to provide projections of sea level patterns are initialised from a long HadCM3 control simulation¹. HadCM3 (Gordon et al., 2000; Pope et al., 2000) is a coupled atmosphere-ocean general circulation model (AOGCM). The atmosphere model has a resolution of 3.75° longitude by 2.5° latitude with 19 vertical levels. The ocean model has a resolution of 1.25° longitude by 1.25° latitude with 20 vertical levels. The sea ice model uses a simple thermodynamic scheme including leads and snow-cover, with ice advected by the surface ocean current. There is no explicit representation of iceberg calving, so a prescribed water flux is returned to the ocean at a rate calibrated to balance the net snowfall accumulation on the ice sheets, geographically distributed within regions where icebergs are found (Gladstone et al., 2001). The ocean model has a rigid lid surface boundary condition with surface freshwater fluxes applied as a virtual salt flux; a reference salinity of 35 psu is used to avoid a global average salinity drift. Changes in sea surface height are calculated in a post-processing step, using the method described by Lowe and Gregory (2006).

The standard HadCM3 control simulation ran for more than two thousand years after initialisation, with the ocean spun-up from rest and with initial potential temperature and salinity data from the World Ocean Atlas (Levitus et al., 1994; Levitus and Boyer, 1994). However, there is a drift with an ocean heat uptake of 0.3 W m^{-2} . The case study scenarios of additional ice-melt used in this study were applied as anomaly fluxes to the HadCM3 model ocean component surface layer for two greenhouse gas scenarios: a simulation with fixed pre-industrial levels of greenhouse gas concentration (appropriate to 1861) and also to a simulation under the SRES A1B greenhouse-gas scenario.

¹The HadCM3 control simulation was continued, for the purposes of providing a baseline simulation for the ice flux scenario simulations: this was necessarily on a new computer platform. This simulation was, however, set up as far as possible to be equivalent to the earlier part of the control simulation and validation supports this.

Dynamic sea level rise pattern from land-ice

T. Howard et al.

Title Page

Abstract

Introduction

Conclusions

References

Tables

Figures



Back

Close

Full Screen / Esc

Printer-friendly Version

Interactive Discussion



Dynamic sea level rise pattern from land-ice

T. Howard et al.

Title Page

Abstract

Introduction

Conclusions

References

Tables

Figures

◀

▶

◀

▶

Back

Close

Full Screen / Esc

Printer-friendly Version

Interactive Discussion



The A1B projection was initialised from the control simulation. The radiative forcing changes appropriate to the period of time-varying greenhouse gas concentration were applied following the methodology of Forster and Taylor (2006), which offers a simplified equivalent A1B forcing in terms of CO₂ alone, diagnosed from the original IPCC Third Assessment Report HadCM3 simulations. We used this CO₂ forcing for our A1B projections, which are otherwise identical to our control run. The 21st century changes in sea surface temperature, salinity and DSL in the northern Atlantic were broadly similar to the climate changes seen under the standard HadCM3 A1B simulation.

As mentioned above, the standard HadCM3 model includes a time-and-scenario invariant flux of freshwater into the oceans in regions around the ice sheets, which represents iceberg calving and melt, and which forms part of the closure of the water budget (Gordon et al., 2000). We leave this term unchanged, as it forms part of the baseline “equilibrium” state of ice-melt-related freshwater flux. The static ice sheets in the model have a dynamic surface mass balance, producing runoff to the ocean, which increases under increased greenhouse gas forcing. The case study scenarios of ice melt we are using, however, incorporate projected anomalies in ice sheet runoff derived from the MAR regional model. To avoid double-accounting of the surface runoff the HadCM3 internal simulation of melt-water runoff is switched off, replacing it with the climatological seasonal cycle derived from the pre-industrial control simulation. The impact of replacing the runoff simulation, on sea surface temperature (SST), sea surface salinity (SSS) and DSL was found to be small compared to the impact of the ice-melt forcing.

Glaciers and small ice caps are not explicitly represented in the coarse resolution HadCM3 model, so the scenario anomalies of freshwater flux from such ice are simply added to the river runoff fluxes.

To compensate for model climate drift, locally or in globally-integrated quantities, a low-pass temporal filter with a 600-yr cut-off is applied to the parallel control simulation. This filtered signal is taken to be the model drift and we take this into account for our analyses (Sect. 4) of changes in DSL and other quantities. However, our results are

not sensitive to omitting this drift compensation, indicating that the amount of drift over this period is small.

HadCM3 simulations have been extensively analysed, with evaluation of the time-mean climatology under fixed forcing for mean ocean quantities (Gordon et al., 2000; Pardaens et al., 2003), and aspects of variability (Vellinga and Wu, 2004). There is a region of cold surface temperature and fresh bias in the northern Atlantic, consistent with a somewhat more zonal flow of the North Atlantic Drift. The distribution of winter sea ice in the high latitude Atlantic shows an extent bias into the Greenland and Barents Seas as described by Gordon et al. (2000).

4 DSL changes induced by scenarios of land-based ice melt under pre-industrial baseline conditions

In this section we present the change in DSL patterns (i.e. excluding global mean sea level changes) which are associated with the MR and HE ice-melt scenarios, under pre-industrial radiative forcing background conditions and under greenhouse-gas warming conditions.

A three member ensemble is generated against which DSL, SSS and SST changes are assessed within the baseline conditions of fixed pre-industrial greenhouse gas concentrations. Using an ensemble allows us to make a more robust assessment of the pattern of change associated with the ice melt, in spite of the presence of considerable unforced variability.

The extent to which the ice-scenario-related pattern of DSL change is different between baseline conditions and those of the forced SRES A1B scenario is also investigated.

The general approach in assessing the simulations is to identify the patterns associated with the mean DSL change over the last 100 yr, when the forcing is strong. The time evolution of the DSL pattern can be regressed against the freshwater fluxes and studied in the light of the corresponding salinity and temperature changes to facilitate

Dynamic sea level rise pattern from land-ice

T. Howard et al.

Title Page

Abstract

Introduction

Conclusions

References

Tables

Figures



Back

Close

Full Screen / Esc

Printer-friendly Version

Interactive Discussion



mechanistic analysis of the change. All analysis is referenced to the concurrent low-pass filtered pre-industrial control simulations to eliminate the model drift.

4.1 Time mean DSL changes

The DSL changes that are robustly associated with the ice scenarios are identified using a time-and-ensemble average, over the final 100 yr of the three member HE ice-melt flux simulations (Fig. 3).

The methodology to identify significant changes is inspired by, but not identical to, that proposed by Livezey and Chen (1983). Significant regions of DSL change in the ensemble-mean (Fig. 3a) are identified using two criteria: (1) the sign of the forced anomalies at each model grid point is the same in all three simulations, and (2) the absolute value of the ensemble-mean change (at each model grid point) is greater than two standard deviations (2σ) of the distribution of 100 yr-mean unforced changes from non-overlapping periods of the control simulation at that grid point. Note that this is a stricter criterion for the ensemble mean than for the individual forced simulations. No significant pattern is found when these same criteria are applied to a mean of the final 100 yr of the concurrent three sections of control simulation.

Substantial areas of significant DSL change are found under the HE ice melt scenario (Fig. 3). For the ensemble mean, these areas are primarily in the North Atlantic, the Arctic and the Southern Ocean. For the North Atlantic the individual ensemble members each give similar patterns of DSL change (Fig. 3b–d). The impact of these regional deviations on local SLR would be relatively small: under the HE scenario, the DSL deviation is of the order of 3 cm in the North Atlantic around NW Europe, for example, while the global-mean SLE of the total HE ice melt is 57 cm. However the magnitude of the DSL response to the freshwater flux forcing is not inconsistent with that found in hosing experiments, once the different levels of freshwater flux are accounted for. For example Swingedouw et al. (2013) show DSL impacts of a 0.1 Sv hosing around Greenland averaged over the fourth decade of hosing for four different models (their Fig. 16). By the middle of that decade, the ocean has received 3.5 Sv years

Dynamic sea level rise pattern from land-ice

T. Howard et al.

Title Page

Abstract

Introduction

Conclusions

References

Tables

Figures



Back

Close

Full Screen / Esc

Printer-friendly Version

Interactive Discussion



of anomalous freshwater forcing from Greenland. Our averaging period is 2000–2099; by the middle of this period our ocean has received only around 0.6 Sv years from Greenland (and about 3 Sv years in total, globally). Taking the minimum-to-maximum sea level height difference in the North Atlantic as a simple measure of the strength of the ocean DSL response, we see responses of around 40 cm (IPSLCM5); 10 cm (MPI-ESM); 25 cm (EC-Earth) and 30 cm (ORCA05) (all values estimated by eye from Swingedouw et al., 2013, their Fig. 16, and disregarding the pattern north of Iceland in IPSLCM5). Our corresponding value is around 8 cm, which does not seem out of place given the weaker forcing in our simulation. Furthermore, disregarding the strength of the response and considering only the spatial pattern, and in spite of the different forcing and averaging periods, our spatial pattern of DSL response in the North Atlantic lies within the envelope of patterns presented by Swingedouw et al. (2013), with a maximum sea-level rise around 45° N, 30° W, and a marked spatial similarity to the pattern of ORCA05 (though with different magnitude, as discussed above).

Our individual ensemble members (Fig. 3b–d) show weak patterns in the tropical Pacific where the variability, on 100 yr timescales, is low. In the Southern Ocean the freshwater input, 95 % of which occurs in the Bellingshausen and Amundsen Seas, west of the Peninsula, leads to a surface freshening (0.9 psu) and stratification of the waters near the coast. The stratification leads to a build-up of advected heat in the intermediate waters down to 1000 m (Fig. 4) leading to a small thermosteric sea level rise. This behaviour is in good agreement in the processes described by Stouffer et al. (2007), with increased incidences of deep convection resulting from the warmer deep waters similar to that found by Keeling and Visbeck (2011). With very little glacial melt in the Weddell Sea region, the stratification there is relatively weak (0.2 psu) until the last decade of the simulation. There is no discernable change in the Antarctic Circumpolar Current (ACC) volume or freshwater transport though the Drake Passage (not shown). However, the barotropic stream function of the Weddell and Ross Sea gyres increases (Fig. 4) which would result in a drop in the sea level within each gyre to maintain

**Dynamic sea level
rise pattern from
land-ice**

T. Howard et al.

Title Page

Abstract

Introduction

Conclusions

References

Tables

Figures

◀

▶

◀

▶

Back

Close

Full Screen / Esc

Printer-friendly Version

Interactive Discussion



geostrophic balance. A fall in DSL does indeed result in the Weddell Sea (Fig. 3) but a similar effect in the Ross Sea is offset by the increase in oceanic heat content.

The ocean stratification around Antarctica leads to a fairly uniform and statistically significant 10% increase in the sea ice cover over the last 50 yr of the simulation.

However, despite a considerable freshwater input to the Southern Ocean late in the timeseries, we do not see a clear link between Southern Ocean and North Atlantic MOC as suggested by Swingedouw et al. (2009). It is possible that the lag in affecting the MOC in HadCM3 is longer than 50 yr and consequently the freshwater input to the Southern Ocean would influence the response of the MOC after the end of the simulation.

The high Arctic also shows a significant fall in DSL, principally in the Beaufort Sea. This is related to an inflow of saline warm water from the Atlantic. The slight warming of near freezing waters results in an increase in density and subsequent fall in DSL.

We now focus on the DSL change in the North Atlantic as a case study, to examine the mechanisms behind the pattern of DSL. The patterns of DSL change in this region are similar in the MR and HE ice melt scenarios (Fig. 5) for the northern Atlantic ensemble mean, but differ in magnitude, with smaller deviations under the MR scenario. The similarity of the patterns in MR and HE scenarios suggests that the pattern is time-invariant with increasing Greenland ice melt; however the low amplitude of the DSL change makes this difficult to robustly identify, as the signal only becomes significant in long-term means.

4.2 Time evolution of DSL changes under the HE ice melt scenario

In order to study the time evolution of the northern Atlantic DSL changes identified as associated with the ice melt scenarios (Sect. 4.1), we project the year-by-year DSL anomaly (denoted $s_i(t)$, where t is year and i is grid point) onto the mean pattern of DSL change (p_i) depicted in Fig. 5a. Given the similarity of the identified DSL pattern changes under HE and MR ice melt scenarios (cf. Fig 5a and b), we here assess only the HE scenario. The projection $\pi(t)$, which can be thought of as the component of p_i

Dynamic sea level rise pattern from land-ice

T. Howard et al.

Title Page

Abstract

Introduction

Conclusions

References

Tables

Figures



Back

Close

Full Screen / Esc

Printer-friendly Version

Interactive Discussion



present in $s_i(t)$, is the scalar product of $s_i(t)$ and normalised ρ_i :

$$\pi(t) = \frac{\text{cov}(s(t), \rho)}{\sqrt{\text{var}(\rho)}} = \frac{\sum s_i(t) \rho_i w_i}{\sqrt{(\sum \rho_i^2 w_i) (\sum w_i)}} \quad (1)$$

The covariance and variance calculations are area-weighted by w_i , the area of grid-point i (Baldwin et al., 2009). Of the three quantities $s_i(t)$, ρ_i and w_i , only $s_i(t)$ changes year to year.

Using $\pi(t)$, the evolution of HE ice-scenario-related DSL anomalies is characterised for each ensemble member (Fig. 6a). The DSL pattern only develops when the Greenland freshwater flux becomes significant (after year 2000, cf. Fig. 1). The forced (before year 2000) and their parallel control simulations show similar weak associations with the pattern suggesting that part of the pattern is associated with a cycle of internal variability in HadCM3. However, the independent samples of the long HadCM3 control simulation show no significant association with the pattern (Fig. 6b). Clearly, however, as the DSL response was defined from the ice-melt scenario simulations, there is some circularity in this procedure. The effect of this circularity can be estimated by following the same procedure with control simulation sections of the same length, i.e. defining an alternative DSL anomaly pattern from these control sections and then assessing its evolution. This test indicates that the circularity effect is a factor which only marginally contributes to the regression (Fig. 6c and d).

The relationship of the evolving ice-melt-associated DSL anomalies in the northern Atlantic (Fig. 5a) with the time-varying ice-melt-scenario-flux, is inferred by comparing with the hemispherically-integrated Northern Hemisphere freshwater anomaly (Fig. 7). Both the gradual increase, and the shorter-term variability, of the ice flux are reflected in the evolving projection of the ensemble-mean DSL pattern (Fig. 7a). There is no clear and notable time-lag between the evolution of the DSL projection and the variations in ice flux. Both the inter-annual to decadal variability and ensemble-spread of the DSL projections are significant compared to the magnitude of the ice-melt-associated DSL pattern.

Dynamic sea level rise pattern from land-ice

T. Howard et al.

Title Page

Abstract

Introduction

Conclusions

References

Tables

Figures



Back

Close

Full Screen / Esc

Printer-friendly Version

Interactive Discussion



4.3 Patterns of change most strongly associated with ice melt changes: North Atlantic

The ice-melt scenario freshwater fluxes have both an underlying increase over the 21st century and substantial shorter-period variability (Fig. 1). An alternative approach to that of Sect. 4.1 for identifying DSL patterns of change associated with the ice melt is to identify locations where the DSL anomalies are strongly correlated with the evolution of the ice melt fluxes: this emphasises the part of the signal that is more strongly associated with the forcing. Such a regression does not explicitly take account of any lag in the response, but the ice-melt fluxes are smoothed before being applied and so contain strong autocorrelation.

The ensemble-average DSL anomaly timeseries fields for the North Atlantic region (80° E to 100° W, 15° N to 90° N) are regressed against the integrated Northern Hemisphere ice-melt fluxes. The significance of the resulting patterns (Fig. 8) is obtained by similarly regressing ensemble-averages of three unforced control simulation sections against the freshwater fluxes (patterns are shown where more than 16 % of the variance in DSL is explained by the freshwater fluxes: cut-off is chosen on the basis that no areas satisfy this condition in our unforced control simulation; about 25 % of the field area satisfies this condition for the ice-melt forced simulation). The resultant pattern (Fig. 8) is spatially similar to that found by considering the 100 yr means in Sect. 4.1 (Fig. 5a). We find that the total Northern Hemisphere freshwater flux is more statistically significant than the global flux in explaining the DSL pattern in this region, indicating a weaker dependence on the Southern Hemisphere flux.

The associated SST and SSS anomalies, identified in the same way, are shown in Figs. 9 and 10, which show that the DSL increase in the Labrador Sea, the sub-polar gyre and the Arctic coastline are associated with a surface freshening. Under stronger, more uniform conditions of northern Atlantic freshwater hosing, similar decreases in SST and SSS in the surrounds of the UK have been found to be associated with freshwater “leakage” from the sub-polar gyre (Swingedouw et al., 2013). The

Dynamic sea level rise pattern from land-ice

T. Howard et al.

Title Page

Abstract

Introduction

Conclusions

References

Tables

Figures



Back

Close

Full Screen / Esc

Printer-friendly Version

Interactive Discussion



Dynamic sea level rise pattern from land-ice

T. Howard et al.

Title Page

Abstract

Introduction

Conclusions

References

Tables

Figures

◀

▶

◀

▶

Back

Close

Full Screen / Esc

Printer-friendly Version

Interactive Discussion



wider patterns of change in North Atlantic SSS and SST are also consistent with, albeit weaker than, those found to be associated with a change in the structure of the sub-polar gyre through freshwater hosing experiments with HadCM3 (Kleinen et al., 2009; Swingedouw et al., 2013). The cooling and freshening in the North Atlantic is suggestive of an expanded sub-polar gyre over the sub-tropical gyre. Some changes in the boundaries of the HadCM3 sub-tropical gyre were discussed by Swingedouw et al. (2013) but these may have been the result of multi-decadal variability rather than a secular trend. Despite the local freshening and warming patterns in the North Atlantic and Barents Sea respectively, there are no significant changes to the sea ice area. The SSS pattern associated with the ice melt is similar to that observed by Hu (2013) in the North Atlantic but their response in the Arctic is of a general freshening rather than the salinification that we observe.

5 Combined greenhouse-gas and enhanced future ice-melt projections of DSL change

The analysis of Sect. 4 focused on the effect of the ice melt scenarios on DSL under conditions of fixed, pre-industrial, greenhouse gas concentrations. Here we assess the patterns of DSL change induced by the HE ice scenario under an SRES A1B radiative forcing scenario (IPCC, 2000). As in Sect. 4, patterns presented in this section exclude any change in the global mean. We use five different individual simulations for our analysis, as indicated in Table 1.

The global pattern of DSL change in HadCM3 under the SRES A1B greenhouse gas scenario without an ice melt scenario (Fig. 11a) shows particular features which have been described and analysed in previous studies (Lowe and Gregory, 2006). As noted in the introduction, different models tend to differ in their pattern and magnitude of DSL change under a common scenario of greenhouse gas warming, but a number of features tend to be more common (Yin, 2012). Common features include, for example, a lower-than-global-mean sea level rise in the Southern Ocean and a

greater-than-global-mean rise off the north east coast of America (Levermann et al., 2005; Yin et al., 2009).

The pattern of DSL change induced by the ice melt scenario alone under A1B greenhouse gas warming conditions is given by differencing the A1B_HE(s) simulation with the A1B(s) simulation (Fig. 11). This change in DSL compares well with that found when the ice melt scenario is applied under pre-industrial greenhouse gas conditions (Fig. 3a). This similarity of pattern of change under different baseline conditions supports a linear addition of the effect on DSL of the ice melt scenarios and of other radiative forcing effects to give a combined pattern of DSL change. Given this linearity, we conclude that it is reasonable to add the DSL change associated with the HE scenario to alternative patterns of DSL change associated with any greenhouse-gas forcing.

6 The role of the MOC in ice-melt induced patterns of DSL change

As noted in the introduction, many previous studies have found links between changes in the Atlantic MOC and patterns of DSL change in the Atlantic. In Sect. 4.3, we noted that the ice-melt related patterns of change in SST and SSS were consistent with those of Swingedouw et al. (2013). They found that the amount of MOC weakening induced by the added freshwater was smaller, when the amount of freshwater that was able to “leak” from the subpolar gyre into the Canary current was larger. In HadCM3, Swingedouw et al. (2013) found that HadCM3 had a relatively large freshwater leakage for the range of models assessed, consistent with relatively little MOC weakening. In this section we estimate the role of Atlantic MOC changes, induced under our ice-melt scenarios, in giving rise to the DSL anomalies we have identified. Given the similarity of the patterns of DSL change under both pre-industrial and greenhouse gas baseline conditions (cf. Sects. 4 and 5), we only analyse this relationship for our pre-industrial ensemble of experiments.

There is considerable low-frequency unforced variability in the MOC apparent in the long control simulation (Fig. 12), as has been described and analysed previously

(Vellinga and Wu, 2004; Jackson and Vellinga, 2013). This variability complicates identification of changes induced by the ice melt scenarios. Comparing MOC changes under the HE scenarios and the concurrent control simulation sections (Fig. 13) suggests the additional HE melt water may be linked to a ~ 1 Sv reduction in MOC strength, but a 3-member ensemble is insufficient to clearly separate this from the unforced variability. We can conclude, however, that any MOC reduction that may be induced by the additional ice melt is no more than ~ 1 Sv, a figure similar to that independently determined from rapid surface melt of a coupled Greenland ice sheet model in HadCM3 (Ridley et al., 2005), where the magnitude of the freshwater flux from Greenland is similar to our HE scenario.

The potential impact of such a reduction in the MOC strength alone on DSL change in the northern Atlantic is inferred from a regression of the control simulation DSL against MOC strength (Fig. 14; which can be scaled to give the pattern for a 1 Sv decrease in MOC strength). The DSL change from the MOC alone is only similar to that from the ice melt scenario (e.g. Fig. 5) in the Labrador Sea and central Arctic, but does not match in the Greenland Sea or the central North and NE Atlantic. Using the unforced control simulation, a regression of the projection parameter $\pi(t)$ (Eq. 1, in this case a projection of the unforced data onto the forced pattern) on the corresponding unforced MOC has a coefficient of -0.8 cm Sv^{-1} . Thus, a 1 Sv decrease in the MOC, which is the order of decrease in MOC that we estimate may be induced by the HE ice melt scenario, might be expected to contribute about 0.8 cm (under an assumption of linearity) of the ~ 2 cm change in the projection parameter, which is the order of change depicted in Fig. 6. We conclude that the impact on DSL of the ice-scenario-induced changes to the MOC is therefore not likely to be the sole contributor to the total ice scenario DSL change.

7 Conclusions

We have used case study 21st century projections of land-based ice melt to investigate the potential dynamical sea level response associated with ice melt alone. We have

Dynamic sea level rise pattern from land-ice

T. Howard et al.

Title Page

Abstract

Introduction

Conclusions

References

Tables

Figures



Back

Close

Full Screen / Esc

Printer-friendly Version

Interactive Discussion



**Dynamic sea level
rise pattern from
land-ice**

T. Howard et al.

Title Page

Abstract

Introduction

Conclusions

References

Tables

Figures



Back

Close

Full Screen / Esc

Printer-friendly Version

Interactive Discussion



created two temporally- and spatially-varying datasets of land-ice melt over the 21st century, one a mid-range scenario and the other representing a high-end scenario. The freshwater datasets include simulated melt from mountain glaciers and ice caps, and input from the major ice sheets. Both the ice sheet surface mass balance and dynamic changes are included, with a component associated with the partial collapse of the west Antarctic ice sheet making an appearance at the end of the 21st century. The scenarios are thus designed to represent potential timelines of land-based freshwater flux into the ocean, rather than being sensitivity studies.

We have incorporated these ice sheet freshwater flux scenarios into simulations using the HadCM3 model, with the additional water inserted into the oceans at coastal grid cells. A simulation including global warming as well as the ice melt scenario shows a similar ice-melt pattern of DSL change from ice melt alone (in addition to the greater magnitude pattern associated with global warming) to that where the baseline conditions are pre-industrial. Despite the majority of the ice melt originating from Antarctica, the largest ice-scenario-induced changes in DSL are in the Arctic and the North Atlantic, with some lesser, but statistically significant, changes around Antarctica. As we have noted, many previous studies have associated changes in North Atlantic DSL with changes in the MOC. Under our case study ice melt scenarios, the effect of the additional freshwater flux on the MOC is small (< 1 Sv). An analysis of the effect of such a low frequency change in MOC on northern Atlantic DSL pattern, using a regression analysis of the long pre-industrial control simulation, suggests that $\sim 60\%$ of the resultant DLS pattern is associated directly with the ice melt.

The mean DSL change is small, perhaps 3 cm in the NW Atlantic, on a level comparable to the unforced variability. Around Antarctica the freshwater input stratifies the ocean, preventing heat transported into the region at intermediate depths (300–700 m) from being released at the surface. This leads to an increase in ocean heat content and a small local sea level rise. A baroclinic change in the Weddell Sea results in a spin-up of the Weddell gyre and a lowering of sea level. Our result is similar in magnitude of DSL rise to a transient simulation with the MIT GCM (Stammer, 2008). That simulation

resulted in a more widespread distribution of water from Greenland melt, with a quite different pattern in the North Atlantic, but a similarly confined impact on the global oceans from Antarctic melt.

Model uncertainty is addressed by comparing our results with a multi-model comparison (Swingedouw et al., 2013) in which the Atlantic pattern of DSL rise was attributed to the magnitude and pathway of freshwater leakage from the subpolar to subtropical gyres. In addition the differences in model asymmetries of the subpolar gyre shape and barotropic stream function, as well as responses of the MOC, contribute to the uncertainty. Large uncertainties were found for the DSL response in the Arctic, and attributed to the transport pathways of Atlantic water, with various effects on the sea ice edge in the Barents Sea.

To summarise, we find that the pattern of DSL change is independent of warming scenario, and appears to scale according to the freshwater input. Consequently, the pattern of ice melt related DSL may be linearly added to other components such as those associated with heat uptake and changes to the hydrological cycle. Thus, in principle any climate model may adopt the pattern, provided it does not double account freshwater with the ice sheet melt from its internal physics.

Acknowledgements. This work was supported by funding from the ice2sea programme from the European Union 7th Framework Programme, grant number 226375. Ice2Sea contribution number #146.

References

- Aiken, C. M. and England, M. H.: Sensitivity of the present-day climate to freshwater forcing associated with Antarctic sea ice loss, *J. Climate*, 21, 3936–3946, doi:10.1175/2007jcli1901.1, 2008.
- Baldwin, M. P., Stephenson, D. B., and Jolliffe, I. T.: Spatial weighting and iterative projection methods for EOFs, *J. Climate*, 22, 234–243, doi:10.1175/2008jcli2147.1, 2009.
- Barrand, N. E., Vaughan, D. G., Steiner, N., Tedesco, M., Munneke, P., van den Broeke, M. R., and Hosking, J. S.: Trends in Antarctic Peninsula surface melting condi-

Dynamic sea level rise pattern from land-ice

T. Howard et al.

Title Page

Abstract

Introduction

Conclusions

References

Tables

Figures



Back

Close

Full Screen / Esc

Printer-friendly Version

Interactive Discussion



Dynamic sea level rise pattern from land-ice

T. Howard et al.

Title Page

Abstract

Introduction

Conclusions

References

Tables

Figures

◀

▶

◀

▶

Back

Close

Full Screen / Esc

Printer-friendly Version

Interactive Discussion



tions from observations and regional climate modelling, *J. Geophys. Res.*, 118, 315–330, doi:10.1029/2012JF002559, 2013.

Bevan, S. L., Luckman, A. J., and Murray, T.: Glacier dynamics over the last quarter of a century at Helheim, Kangerdlugssuaq and 14 other major Greenland outlet glaciers, *The Cryosphere*, 6, 923–937, doi:10.5194/tc-6-923-2012, 2012.

Bindschadler, R.: Hitting the ice sheets where it hurts, *Science*, 311, 1720–1721, doi:10.1126/science.1125226, 2006.

Bindschadler, R. A., Nowicki, S., Abe-Ouchi, A., Aschwanden, A., Choi, H., Fastook, J., Granzow, G., Greve, R., Gutowski, G., Herzfeld, U., Jackson, C., Johnson, J., Kroulev, C., Levermann, A., Lipsomb, W., Martin, M., Morlighem, M., Parizek, B., Pollard, D., Price, S., Ren, D., Saito, F., Sato, T., Seddik, H., Seroussi, H., Takahashi, K., Walker, R., and Wang, W. L.: Ice-sheet model sensitivities to environmental forcing and their use in projecting future sea level (the SeaRISE project), *J. Glaciol.*, 59, 195–224, 2013.

Bingham, R. J. and Hughes, C. W.: Signature of the Atlantic meridional overturning circulation in sea level along the east coast of North America, *Geophys. Res. Lett.*, 36, L02603, doi:10.1029/2008GL036215, 2009.

Christoffersen, P., Mugford, R. I., Heywood, K. J., Joughin, I., Dowdeswell, J. A., Syvitski, J. P. M., Luckman, A., and Benham, T. J.: Warming of waters in an East Greenland fjord prior to glacier retreat: mechanisms and connection to large-scale atmospheric conditions, *The Cryosphere*, 5, 701–714, doi:10.5194/tc-5-701-2011, 2011.

Church, J. A., Woodworth, P. L., Aarup, T., and Wildon, W. S.: Understanding sea-level rise and variability, 428 pp., Chichester, Wiley-Blackwell, 2010.

Church, J. A., White, N. J., Konikow, L. F., Domingues, C. M., Cogley, J. G., Rignot, E., Gregory, J. M., van den Broeke, M. R., Monaghan, A. J., and Velicogna, I.: Revisiting the Earth's sea-level and energy budgets from 1961 to 2008, *Geophys. Res. Lett.*, 38, L18601, doi:10.1029/2011gl048794, 2011.

Cornford, S. L., Martin, D. F., Graves, D. T., Ranken, D. F., Le Brocq, A. M., Gladstone, R. M., Payne, A. J., Ng, E. G., and Lipscomb, W. H.: Adaptive mesh, finite volume modelling of marine ice sheets, *J. Comput. Phys.*, 232, 529–549, doi:10.1016/j.jcp.2012.08.037, 2013.

Cunningham, S. A., Kanzow, T., Rayner, D., Baringer, M. O., Johns, W. E., Marotzke, J., Longworth, H. R., Grant, E. M., Hirschi, J. J. M., Beal, L. M., Meinen, C. S., and Bryden, H. L.: Temporal variability of the Atlantic meridional overturning circulation at 26.5° N, *Science*, 317, 935–938, doi:10.1126/science.1141304, 2007.

Dynamic sea level rise pattern from land-ice

T. Howard et al.

Title Page

Abstract

Introduction

Conclusions

References

Tables

Figures

◀

▶

◀

▶

Back

Close

Full Screen / Esc

Printer-friendly Version

Interactive Discussion



- Doake, C. S. M. and Vaughan, D. G.: Rapid disintegration of the Wordie ice shelf in response to atmospheric warming, *Nature*, 350, 328–330, doi:10.1038/350328a0, 1991.
- Drijfhout, S. S., Weber, S. L., and van der Swaluw, E.: The stability of the MOC as diagnosed from model projections for pre-industrial, present and future climates, *Clim. Dynam.*, 37, 1575–1586, doi:10.1007/s00382-010-0930-z, 2011.
- Fettweis, X.: Reconstruction of the 1979–2006 Greenland ice sheet surface mass balance using the regional climate model MAR, *The Cryosphere*, 1, 21–40, doi:10.5194/tc-1-21-2007, 2007.
- Forster, P. M. D. and Taylor, K. E.: Climate forcings and climate sensitivities diagnosed from coupled climate model integrations, *J. Climate*, 19, 6181–6194, doi:10.1175/jcli3974.1, 2006.
- Fürst, J. J., Goelzer, H., and Huybrechts, P.: Effect of higher-order stress gradients on the centennial mass evolution of the Greenland ice sheet, *The Cryosphere*, 7, 183–199, doi:10.5194/tc-7-183-2013, 2013.
- Giesen, R. H. and Oerlemans, J.: Calibration of a surface mass balance model for global-scale applications, *The Cryosphere*, 6, 1463–1481, doi:10.5194/tc-6-1463-2012, 2012.
- Gillet-Chaulet, F., Gagliardini, O., Seddik, H., Nodet, M., Durand, G., Ritz, C., Zwinger, T., Greve, R., and Vaughan, D. G.: Greenland ice sheet contribution to sea-level rise from a new-generation ice-sheet model, *The Cryosphere*, 6, 1561–1576, doi:10.5194/tc-6-1561-2012, 2012.
- Gladstone, R. M., Bigg, G. R., and Nicholls, K. W.: Iceberg trajectory modeling and melt-water injection in the Southern Ocean, *J. Geophys. Res.-Ocean.*, 106, 19903–19915, doi:10.1029/2000jc000347, 2001.
- Gordon, C., Cooper, C., Senior, C. A., Banks, H., Gregory, J. M., Johns, T. C., Mitchell, J. F. B., and Wood, R. A.: The simulation of SST, sea ice extents and ocean heat transports in a version of the Hadley Centre coupled model without flux adjustments, *Clim. Dynam.*, 16, 147–168, doi:10.1007/s003820050010, 2000.
- Goelzer, H., Huybrechts, P., Fürst, J. J., Andersen, M. L., Edwards, T. L., Fettweis, X., Nick, F. M., Payne, A. J., and Shannon, S.: Sensitivity of Greenland ice sheet projections to model formulations, *J. Glaciol.*, 59, 733–749, doi:10.3189/2013JoG12J182, 2013.
- Graversen, R. G., Drijfhout, S., Hazeleger, W., van de Wal, R., Bintanja, R., and Helsen, M.: Greenland's contribution to global sea level rise by the end of the 21st century, *Clim. Dynam.*, 37, 1427–1442, 2011.

Dynamic sea level rise pattern from land-ice

T. Howard et al.

Title Page

Abstract

Introduction

Conclusions

References

Tables

Figures

◀

▶

◀

▶

Back

Close

Full Screen / Esc

Printer-friendly Version

Interactive Discussion



- Gregory, J. M., Dixon, K. W., Stouffer, R. J., Weaver, A. J., Driesschaert, E., Eby, M., Fichet, T., Hasumi, H., Hu, A., Jungclaus, J. H., Kamenkovich, I. V., Levermann, A., Montoya, M., Murakami, S., Nawrath, S., Oka, A., Sokolov, A. P., and Thorpe, R. B.: A model intercomparison of changes in the Atlantic thermohaline circulation in response to increasing atmospheric CO₂ concentration, *Geophys. Res. Lett.*, 32, L12703, doi:10.1029/2005gl023209, 2005.
- Hakkinen, S. and Rhines, P. B.: Decline of subpolar North Atlantic circulation during the 1990s, *Science*, 304, 555–559, doi:10.1126/science.1094917, 2004.
- Hellmer, H. H., Kauker, F., Timmermann, R., Determann, J., and Rae, J.: Twenty-first-century warming of a large Antarctic ice-shelf cavity by a redirected coastal current, *Nature*, 485, 225–228, doi:10.1038/nature11064, 2012.
- Holland, D. M., Thomas, R. H., De Young, B., Ribergaard, M. H., and Lyberth, B.: Acceleration of Jakobshavn Isbrae triggered by warm subsurface ocean waters, *Nat. Geosci.*, 1, 659–664, doi:10.1038/ngeo316, 2008.
- Hu, A. X., Meeh, G. A., Han, W. Q., and Yin, J. J.: Transient response of the MOC and climate to potential melting of the Greenland Ice Sheet in the 21st century, *Geophys. Res. Lett.*, 36, L10707, doi:10.1029/2009gl037998, 2009.
- Hu, A. X., Meehl, G. A., Han, W. Q., and Yin, J. J.: Effect of the potential melting of the Greenland ice sheet on the Meridional Overturning Circulation and global climate in the future, *Deep-Sea Res. Pt. II*, 58, 1914–1926, doi:10.1016/j.dsr2.2010.10.069, 2011.
- Hu, A. X., Meehl, G. A., Han, W. Q., Yin, J. J., Wu, B. Y., and Kimoto, M.: Influence of continental ice retreat on future global climate, *J. Climate*, 26, 3087–3111, doi:10.1175/JCLI-D-12-00102.1, 2013.
- IPCC, Nakićenović, N. and Swart, R. (Eds.): Special Report on Emissions Scenarios. A Special Report of Working Group III of the Intergovernmental Panel on Climate Change, Cambridge University Press, Cambridge, United Kingdom and New York, NY, USA, 599 pp., 2000.
- Jackson, L. and Vellinga, M.: Multidecadal to centennial variability of the AMOC: HadCM3 and a perturbed physics ensemble, *J. Climate*, 26, 2390–2407, doi:10.1175/JCLI-D-11-00601.1, 2013.
- Jacobs, S. S., Helmer, H. H., Doake, C. S. M., Jenkins, A., and Frolich, R. M.: Melting of ice shelves and the mass balance of antarctica, *J. Glaciol.*, 38, 375–387, 1992.
- Keeling, R. F. and Visbeck, M.: On the linkage between Antarctic surface water stratification and global deep-water temperature, *J. Climate*, 24, 3545–3557, doi:10.1175/2011JCLI3642.1, 2011.

Dynamic sea level rise pattern from land-ice

T. Howard et al.

Title Page

Abstract

Introduction

Conclusions

References

Tables

Figures

◀

▶

◀

▶

Back

Close

Full Screen / Esc

Printer-friendly Version

Interactive Discussion



Kleinen, T., Osborn, T. J., and Briffa, K. R.: Sensitivity of climate response to variations in freshwater hosing location, *Ocean Dynam.*, 59, 509–521, doi:10.1007/s10236-009-0189-2, 2009.

5 Kopp, R. E., Mitrovica, J. X., Griffies, S. M., Yin, J. J., Hay, C. C., and Stouffer, R. J.: The impact of Greenland melt on local sea levels: a partially coupled analysis of dynamic and static equilibrium effects in idealized water-hosing experiments A letter, *Clim. Change*, 103, 619–625, doi:10.1007/s10584-010-9935-1, 2010.

Levermann, A. and Born, A.: Bistability of the Atlantic subpolar gyre in a coarse-resolution climate model, *Geophys. Res. Lett.*, 34, L24605, doi:10.1029/2007gl031732, 2007.

10 Levermann, A., Griesel, A., Hofmann, M., Montoya, M., and Rahmstorf, S.: Dynamic sea level changes following changes in the thermohaline circulation, *Clim. Dynam.*, 24, 347–354, doi:10.1007/s00382-004-0505-y, 2005.

Levitus, S. R. and Boyer, T.: *World Ocean Atlas 1994, vol. 4: Temperature*, NOAA Atlas NESDIS 4, US Gov. Printing Office, Wash., D.C., 117 pp., 1994.

15 Levitus, S. R., Burgett, T., and Boyer, T.: *World Ocean Atlas 1994, vol. 3: Salinity*, NOAA Atlas NESDIS 3, US Gov. Printing Office, Wash., D.C., 99 pp., 1994.

Livezey, R. E. and Chen, W. Y.: Statistical field significance and its determination by Monte Carlo techniques, *Mon. Weather Rev.*, 111, 46–59, doi:10.1175/1520-0493(1983)111<0046:SFSaid>2.0.CO;2, 1983.

20 Lohmann, K., Drange, H., and Bentsen, M.: Response of the North Atlantic subpolar gyre to persistent North Atlantic oscillation like forcing, *Clim. Dynam.*, 32, 273–285, doi:10.1007/s00382-008-0467-6, 2009.

Lorbacher, K., Dengg, J., Böning, C. W., and Biastoch, A.: Regional patterns of sea level change related to interannual variability and multidecadal trends in the Atlantic Meridional Overturning Circulation, *J. Climate*, 23, 4243–4254, doi:10.1175/2010JCLI3341.1, 2010.

25 Lorbacher, K., Marsland, S. J., Church, J. A., Griffies, S. M., and Stammer, D.: Rapid barotropic sea level rise from ice sheet melting, *J. Geophys. Res.*, 117, C06003, doi:10.1029/2011JC007733, 2012.

Lowe, J. A. and Gregory, J. M.: Understanding projections of sea level rise in a Hadley Centre coupled climate model, *J. Geophys. Res.-Oceans*, 111, C11, doi:10.1029/2005JC003421, 2006.

30 Lowe, J. A., Howard, T. P., Pardaens, A., Tinker, J., Holt, J., Wakelin, S., Milne, G., Leake, J., Wolf, J., Horsburgh, K., Reeder, T., Jenkins, G., Ridley, J., Dye, S., and Bradley, S.: UK

Dynamic sea level rise pattern from land-ice

T. Howard et al.

Title Page

Abstract

Introduction

Conclusions

References

Tables

Figures

◀

▶

◀

▶

Back

Close

Full Screen / Esc

Printer-friendly Version

Interactive Discussion

Climate Projections science report: marine and coastal projections, Met Office Hadley Centre, Exeter, UK, available at: <http://ukclimateprojections.defra.gov.uk> (last access: 20 December 2012), 2009.

Marzeion, B., Jarosch, A. H., and Hofer, M.: Past and future sea-level change from the surface mass balance of glaciers, *The Cryosphere*, 6, 1295–1322, doi:10.5194/tc-6-1295-2012, 2012.

McGrath, D., Steffen, K., Rajaram, H., Scambos, T., Abdalati, W., and Rignot, E.: Basal crevasses on the Larsen C ice shelf, Antarctica: implications for meltwater ponding and hydrofracture, *Geophys. Res. Lett.*, 39, L16504, doi:10.1029/2012GL052413, 2012.

Meehl, G. A., Stocker, T. F., Collins, W. D., Friedlingstein, P., Gaye, A. T., Gregory, J. M., Kitoh, A., Knutti, R., Murphy, J. M., Noda, A., Raper, S. C. B., Watterson, I. G., Weaver, A. J., and Zhao, Z.: Global climate projections, in: *Climate Change 2007: the Physical Science Basis*, Contribution of Working Group I to the Fourth Assessment Report of the Intergovernmental Panel on Climate Change, edited by: Solomon, S., Qin, D., Manning, M., Chen, Z., Marquis, M., Averyt, K. B., Tignor, M., and Miller, H. L., Cambridge University Press, London, 2007.

Meier, M. F. and Post, A.: Fast tidewater glacier, *J. Geophys. Res.-Solid*, 92, 9051–9058, doi:10.1029/JB092iB09p09051, 1987.

Meier, M. F., Dyurgerov, M. B., Rick, U. K., O’Neel, S., Pfeffer, W. T., Anderson, R. S., Anderson, S. P., and Glazovsky, A. F.: Glaciers dominate eustatic sea-level rise in the 21st century, *Science*, 317, 1064–1067, doi:10.1126/science.1143906, 2007.

Mikolajewicz, U., Vizcaino, M., Jungclaus, J., and Schurgers, G.: Effect of ice sheet interactions in anthropogenic climate change simulations, *Geophys. Res. Lett.*, 34, L18706, doi:10.1029/2007gl031173, 2007.

Milne, G. A., Gehrels, W. R., Hughes, C. W., and Tamisiea, M. E.: Identifying the causes of sea-level change, *Nat. Geosci.*, 2, 471–478, 2009.

Mitrovica, J. X., Tamisiea, M. E., Davis, J. L., and Milne, G. A.: Recent mass balance of polar ice sheets inferred from patterns of global sea-level change, *Nature*, 409, 1026–1029, doi:10.1038/35059054, 2001.

Nicholls, R. J., Marinova, N., Lowe, J. A., Brown, S., Vellinga, P., De Gusmao, D., Hinkel, J., and Tol, R. S. J.: Sea-level rise and its possible impacts given a “beyond 4 °C world” in the twenty-first century, *Philos. T. Roy. Soc. A*, 369, 161–181, doi:10.1098/rsta.2010.0291, 2011.

Dynamic sea level rise pattern from land-ice

T. Howard et al.

Title Page

Abstract

Introduction

Conclusions

References

Tables

Figures

◀

▶

◀

▶

Back

Close

Full Screen / Esc

Printer-friendly Version

Interactive Discussion



Nick, F. M., Vieli, A., Andersen, M. L., Joughin, I. R., Payne, A. J., Edwards, T., Pattyn, F., and van der Wal, R.: Future sea level rise from Greenland's major outlet glaciers in a warming climate, *Nature*, 497, 235–238, 2013.

Nowicki, S., Bindschadler, R., Abe-Ouchi, A., Aschwanden, A., Bueler, E., Choi, H., Fastook, J., Granzow, G., Greve, R., Gutowski, G., Herzfeld, U., Jackson, C., Johnson, J., Kroulev, C., Larour, E., Levermann, A., Lipsomb, W., Martin, M., Morlighem, M., Parizek, B., Pollard, D., Price, S., Rignot, E., Ren, D., Saito, F., Sato, T., Seddik, H., Seroussi, H., Takahashi, K., Walker, R., and Wang, W. L.: Insights into spatial sensitivities of ice mass response to environmental change from the SeaRISE ice sheet modeling project – I. Antarctica, *J. Geophys. Res.*, 118, 1002–1024, 2013a.

Nowicki, S., Bindschadler, R., Abe-Ouchi, A., Aschwanden, A., Bueler, E., Choi, H., Fastook, J., Granzow, G., Greve, R., Gutowski, G., Herzfeld, U., Jackson, C., Johnson, J., Kroulev, C., Larour, E., Levermann, A., Lipsomb, W., Martin, M., Morlighem, M., Parizek, B., Pollard, D., Price, S., Rignot, E., Ren, D., Saito, F., Sato, T., Seddik, H., Seroussi, H., Takahashi, K., Walker, R., and Wang, W. L.: Insights into spatial sensitivities of ice mass response to environmental change from the SeaRISE ice sheet modeling project – II. Greenland, *J. Geophys. Res.*, 118, 1025–1044, 2013b.

Pardaens, A. K., Banks, H. T., Gregory, J. M., and Rowntree, P. R.: Freshwater transports in HadCM3, *Clim. Dynam.*, 21, 177–195, doi:10.1007/s00382-003-0324-6, 2003.

Pardaens, A. K., Gregory, J. M., and Lowe, J. A.: A model study of factors influencing projected changes in regional sea level over the twenty-first century, *Clim. Dynam.*, 36, 2015–2033, doi:10.1007/s00382-009-0738-x, 2011.

Pattyn, F., Schoof, C., Perichon, L., Hindmarsh, R. C. A., Bueler, E., de Fleurian, B., Durand, G., Gagliardini, O., Gladstone, R., Goldberg, D., Gudmundsson, G. H., Huybrechts, P., Lee, V., Nick, F. M., Payne, A. J., Pollard, D., Rybak, O., Saito, F., and Vieli, A.: Results of the Marine Ice Sheet Model Intercomparison Project, MISMIIP, *The Cryosphere*, 6, 573–588, doi:10.5194/tc-6-573-2012, 2012.

Pfeffer, W. T., Harper, J. T., and O'Neel, S.: Kinematic constraints on glacier contributions to 21st-century sea-level rise, *Science*, 321, 1340–1343, doi:10.1126/science.1159099, 2008.

Pope, V. D., Gallani, M. L., Rowntree, P. R., and Stratton, R. A.: The impact of new physical parametrizations in the Hadley Centre climate model: HadAM3, *Clim. Dynam.*, 16, 123–146, doi:10.1007/s003820050009, 2000.

**Dynamic sea level
rise pattern from
land-ice**

T. Howard et al.

Title Page

Abstract

Introduction

Conclusions

References

Tables

Figures

◀

▶

◀

▶

Back

Close

Full Screen / Esc

Printer-friendly Version

Interactive Discussion



Price, S. F., Payne, A. J., Howat, I. M., and Smith, B. E.: Committed sea-level rise for the next century from Greenland ice sheet dynamics during the past decade, *P. Natl. Acad. Sci. USA*, 108, 8978–8983, doi:10.1073/pnas.1017313108, 2011.

Pritchard, H. D., Arthern, R. J., Vaughan, D. G., and Edwards, L. A.: Extensive dynamic thinning on the margins of the Greenland and Antarctic ice sheets, *Nature*, 461, 971–975, doi:10.1038/nature08471, 2009.

Pritchard, H. D., Ligtenberg, S. R. M., Fricker, H. A., Vaughan, D. G., van den Broeke, M. R., and Padman, L.: Antarctic ice-sheet loss driven by basal melting of ice shelves, *Nature*, 484, 502–505, doi:10.1038/nature10968, 2012.

Radic, V. and Hock, R.: Regionally differentiated contribution of mountain glaciers and ice caps to future sea-level rise, *Nat. Geosci.*, 4, 91–94, doi:10.1038/ngeo1052, 2011.

Rahmstorf, S.: On the freshwater forcing and transport of the Atlantic thermohaline circulation, *Clim. Dynam.*, 12, 799–811, doi:10.1007/s003820050144, 1996.

Rayner, N. A., Parker, D. E., Horton, E. B., Folland, C. K., Alexander, L. V., Rowell, D. P., Kent, E. C., and Kaplan, A.: Global analyses of sea surface temperature, sea ice, and night marine air temperature since the late nineteenth century, *J. Geophys. Res.-Atmos.*, 108, 4407, doi:10.1029/2002jd002670, 2003.

Richardson, G., Wadley, M. R., Heywood, K. J., Stevens, D. P., and Banks, H. T.: Short-term climate response to a freshwater pulse in the Southern Ocean, *Geophys. Res. Lett.*, 32, L03702, doi:10.1029/2004GL021586, 2005.

Ridley, J. K., Huybrechts, P., Gregory, J. M., and Lowe, J. A.: Elimination of the Greenland ice sheet in a high CO₂ climate, *J. Climate*, 18, 3409–3427, doi:10.1175/jcli3482.1, 2005.

Ritz, C., Durand, G., Edwards, T. L., Payne, A. J., Peyaud, V., Richard, C. A., and Hindmarsh, R. C. A.: Bimodal probability of the dynamic contribution of Antarctica to future sea level, *Nature*, submitted, 2013.

Russell, G. L., Gornitz, V., and Miller, J. R.: Regional sea level changes projected by the NASA/GISS Atmosphere-Ocean Model, *Clim. Dynam.*, 16, 789–797, doi:10.1007/s003820000090, 2000.

Schmittner, A., Latif, M., and Schneider, B.: Model projections of the North Atlantic thermohaline circulation for the 21st century assessed by observations, *Geophys. Res. Lett.*, 32, L23710, doi:10.1029/2005GL024368, 2005.

Schoof, C.: Marine ice-sheet dynamics, Part 1: The case of rapid sliding, *J. Fluid Mech.*, 573, 27–55, doi:10.1017/s0022112006003570, 2007.

Dynamic sea level rise pattern from land-ice

T. Howard et al.

Title Page

Abstract

Introduction

Conclusions

References

Tables

Figures

◀

▶

◀

▶

Back

Close

Full Screen / Esc

Printer-friendly Version

Interactive Discussion



Seddik, H., Greve, R., Zwinger, T., Gillet-Chaulet, F., and Gagliardini, O.: Simulations of the Greenland ice sheet 100 yr into the future with the full Stokes model Elmer/Ice, *J. Glaciol.*, 58, 427–440, doi:10.3189/2012JoG11J177, 2012.

Stammer, D.: Response of the global ocean to Greenland and Antarctic ice melting, *J. Geophys. Res.-Oceans*, 113, C06022, doi:10.1029/2006jc004079, 2008.

Stanton, T. P., Shaw, W. J., Truffer, M., Corr, H. F. J., Peters, L. E., Riverman, K. L., Bind-schadler, R., Holland, D. M., and Anandakrishnan, S.: Channelized ice melting in the ocean boundary layer beneath Pine Island glacier, Antarctica, *Science*, 341, 1236–1239, doi:10.1126/science.1239373, 2013.

Stouffer, R. J., Yin, J., Gregory, J. M., Dixon, K. W., Spelman, M. J., Hurlin, W., Weaver, A. J., Eby, M., Flato, G. M., Hasumi, H., Hu, A., Jungclaus, J. H., Kamenkovich, I. V., Levermann, A., Montoya, M., Murakami, S., Nawrath, S., Oka, A., Peltier, W. R., Robitaille, D. Y., Sokolov, A., Vettoretti, G., and Weber, S. L.: Investigating the causes of the response of the thermohaline circulation to past and future climate changes, *J. Climate*, 19, 1365–1387, doi:10.1175/jcli3689.1, 2006.

Stouffer, R. J., Seidov, D., and Haupt, B. J.: Climate response to external sources of freshwater: North Atlantic versus the Southern Ocean, *J. Climate*, 20, 436–448, doi:10.1175/jcli4015.1, 2007.

Swingedouw, D., Fichefet, T., Huybrechts, P., Goosse, H., Driesschaert, E., and Loutre, M.-F.: Antarctic ice-sheet melting provides negative feedbacks on future climate warming, *Geophys. Res. Lett.*, 35, L17705, doi:10.1029/2008GL034410, 2008.

Swingedouw, D., Fichefet, T., Goosse, H., and Loutre, M. F.: Impact of transient freshwater releases in the Southern Ocean on the AMOC and climate, *Clim. Dynam.*, 33, 365–381, doi:10.1007/s00382-008-0496-1, 2009.

Swingedouw, D., Rodehacke, C. B., Behrens, E., Menary, M., Olsen, S. M., Gao, Y., Mikolajewicz, U., Mignot, J., and Biastoch, A.: Decadal fingerprints of freshwater discharge around Greenland in a multi-model ensemble, *Clim. Dynam.*, 41, 695–720, doi:10.1007/s00382-012-1479-9, 2013.

Timmermann, R., Wang, Q., and Hellmer, H. H.: Ice-shelf basal melting in a global finite-element sea-ice/ice-shelf/ocean model, *Ann. Glaciol.*, 53, 303–314, doi:10.3189/2012AoG60A156, 2012.

Van den Broeke, M. R., Bamber, J., Lenaerts, J., and Rignot, E.: Ice sheets and sea level: thinking outside the box, *Surv. Geophys.*, 32, 495–505, doi:10.1007/s10712-011-9137-z, 2011.

Dynamic sea level rise pattern from land-ice

T. Howard et al.

Title Page

Abstract

Introduction

Conclusions

References

Tables

Figures

◀

▶

◀

▶

Back

Close

Full Screen / Esc

Printer-friendly Version

Interactive Discussion



- Vellinga, M. and Wu, P. L.: Low-latitude freshwater influence on centennial variability of the Atlantic thermohaline circulation, *J. Climate*, 17, 4498–4511, doi:10.1175/3219.1, 2004.
- Wang, X., Wang, Q., Sidorenko, D., Danilov, S., Schroter, J., and Jung, T.: Long-term ocean simulations in FESOM: evaluation and application in studying the impact of Greenland ice sheet melting, *Ocean Dynam.*, 62, 1471–1486, doi:10.1007/s10236-012-0572-2, 2012.
- 5 Weaver, A. J., Saenko, O. A., Clark, P. U., and Mitrovica, J. X.: Meltwater pulse 1A from Antarctica as a trigger of the Bolling–Allerod warm interval, *Science*, 299, 1709–1713, doi:10.1126/science.1081002, 2003.
- Weaver, A. J., Sedláček, J., Eby, M., Alexander, K., Crespin, E., Fichefet, T., Philippon-Berthier, G., Joos, F., Kawamiya, M., Matsumoto, K., Steinacher, M., Tachiiri, K., Tokos, K., Yoshimori, M., and Zickfeld, K.: Stability of the Atlantic meridional overturning circulation: a model intercomparison, *Geophys. Res. Lett.*, 39, L20709, doi:10.1029/2012GL053763, 2012.
- 10 Yin, J.: Century to multi-century sea level rise projections from CMIP5 models, *Geophys. Res. Lett.*, 39, L17709, doi:10.1029/2012GL052947, 2012.
- 15 Yin, J., Schlesinger, M. E., and Stouffer, R. J.: Model projections of rapid sea-level rise on the northeast coast of the United States, *Nat. Geosci.*, 2, 262–266, doi:10.1038/ngeo462, 2009.

Dynamic sea level rise pattern from land-ice

T. Howard et al.

Title Page

Abstract

Introduction

Conclusions

References

Tables

Figures

◀

▶

◀

▶

Back

Close

Full Screen / Esc

Printer-friendly Version

Interactive Discussion



Table 1. Simulations used to assess suitability of linear addition of DSL changes.

Climate	Ice melt anomaly	Baseline ice melt
A1B(m)	no ice-melt scenario	model-generated runoff
A1B(s)	no ice-melt scenario	PI climatology
PI(s)	no ice-melt scenario	PI climatology
PI_HE(s)	HE ice melt scenario	PI climatology
A1B_HE(s)	HE ice melt scenario	PI climatology

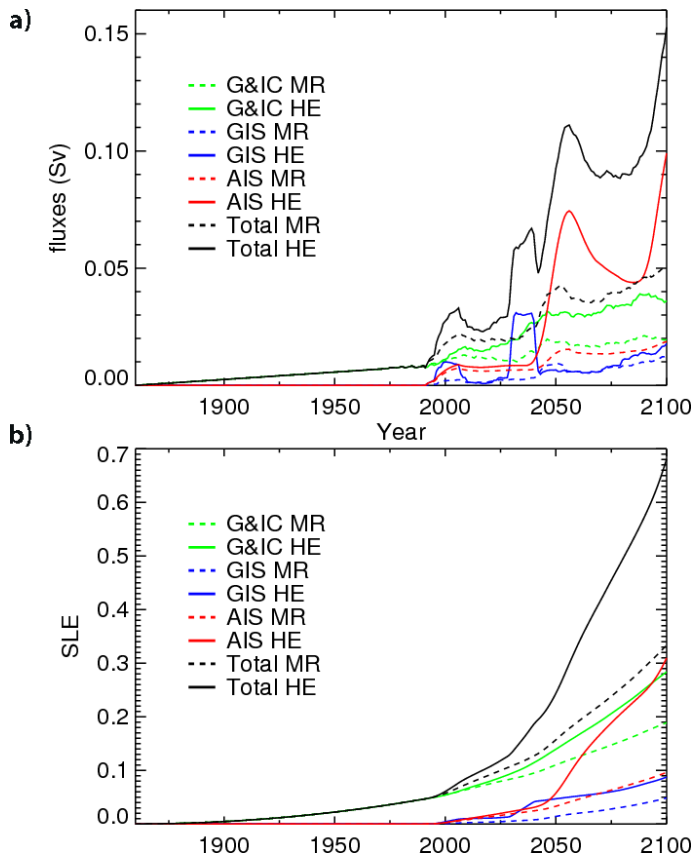


Fig. 1. Global-mean freshwater fluxes from land-based ice masses. **(a)** in Sv **(b)** cumulative, in sea level equivalent (SLE; in m). Note that some part of the ice which is melted is displacing water prior to melt, so while it contributes to the freshwater into the ocean, it would not contribute to sea-level rise. The actual contribution to sea-level rise from the fluxes may therefore be less than the SLE of **(b)**.

**Dynamic sea level
rise pattern from
land-ice**

T. Howard et al.

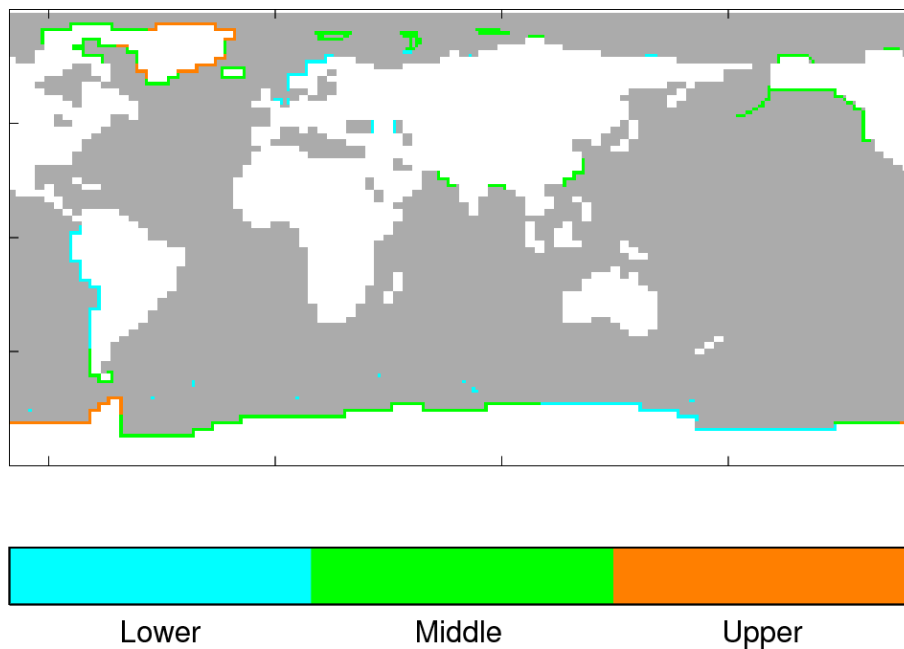


Fig. 2. Ocean grid points involved in freshwater forcing by tercile of integrated freshwater flux (coloured), other ocean grid points (grey) and land grid points (white).

[Title Page](#)[Abstract](#)[Introduction](#)[Conclusions](#)[References](#)[Tables](#)[Figures](#)[◀](#)[▶](#)[◀](#)[▶](#)[Back](#)[Close](#)[Full Screen / Esc](#)[Printer-friendly Version](#)[Interactive Discussion](#)

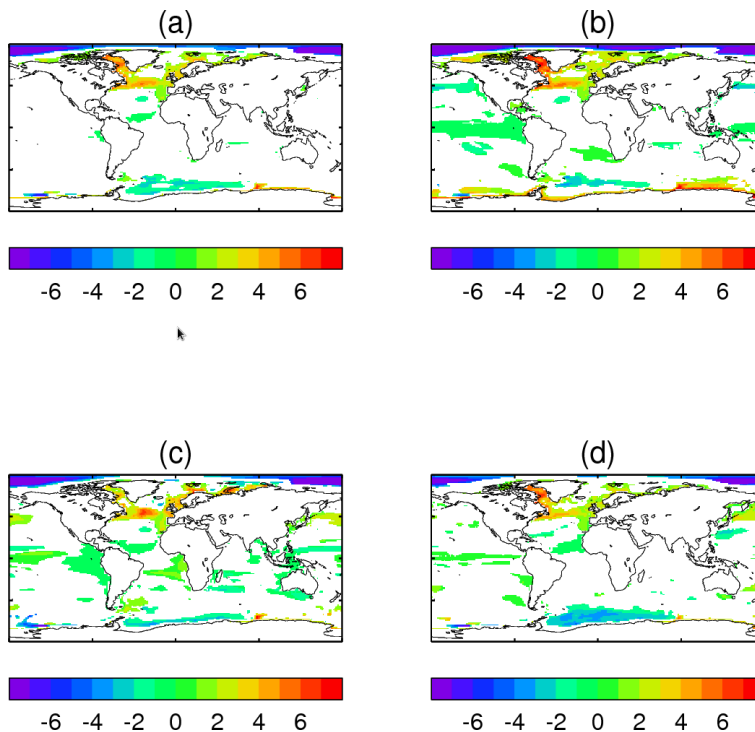


Fig. 3. DSL anomalies (cm) under the HE ice-melt scenario and for pre-industrial baseline conditions, averaged over years 2000–2099. Anomalies are relative to the concurrent period of the low-pass filtered control as described in the main text. **(a)** mean of the three forced simulations. **(b–d)** show the three simulations separately. Coloured regions show where anomalies are greater than 2σ of the distribution from the control simulation. A stricter criterion is applied to panel **(a)**: see main text. Note that the patterns shown are anomalies in two senses: first because they are relative to the concurrent period of the low-pass filtered control and secondly because they exclude any change in the global mean sea level.

Dynamic sea level rise pattern from land-ice

T. Howard et al.

Title Page

Abstract Introduction

Conclusions References

Tables Figures

⏪ ⏩

◀ ▶

Back Close

Full Screen / Esc

Printer-friendly Version

Interactive Discussion



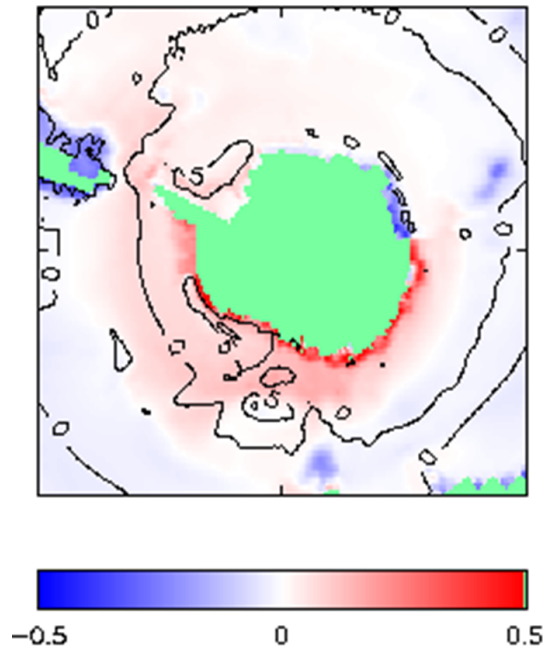


Fig. 4. The changes around Antarctica of mean ocean temperature (colour) and barotropic stream function (contours in Sv). Anomalies are the ice-melt ensemble mean for the last 40 yr reference to the equivalent years of their unforced control simulations.

Dynamic sea level rise pattern from land-ice

T. Howard et al.

Title Page

Abstract Introduction

Conclusions References

Tables Figures

◀ ▶

◀ ▶

Back Close

Full Screen / Esc

Printer-friendly Version

Interactive Discussion



**Dynamic sea level
rise pattern from
land-ice**

T. Howard et al.

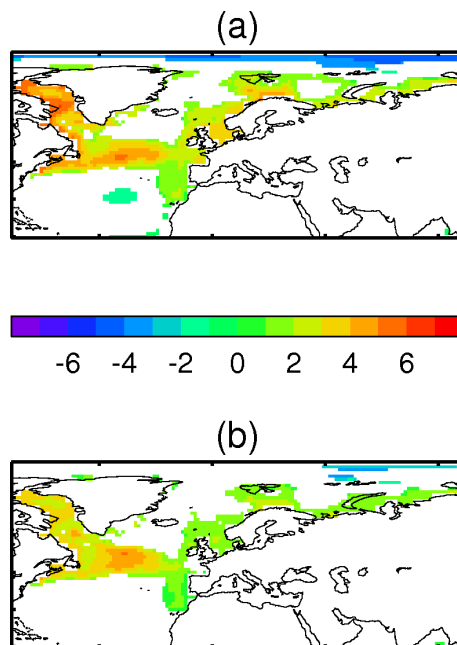


Fig. 5. (a) Ensemble-mean significant DSL anomalies (cm) in the northern Atlantic (a) for HE ice-melt scenario, as Fig. 3a, but showing detail of the northern Atlantic. (b) For MR ice-melt scenario.

[Title Page](#)[Abstract](#)[Introduction](#)[Conclusions](#)[References](#)[Tables](#)[Figures](#)[◀](#)[▶](#)[◀](#)[▶](#)[Back](#)[Close](#)[Full Screen / Esc](#)[Printer-friendly Version](#)[Interactive Discussion](#)

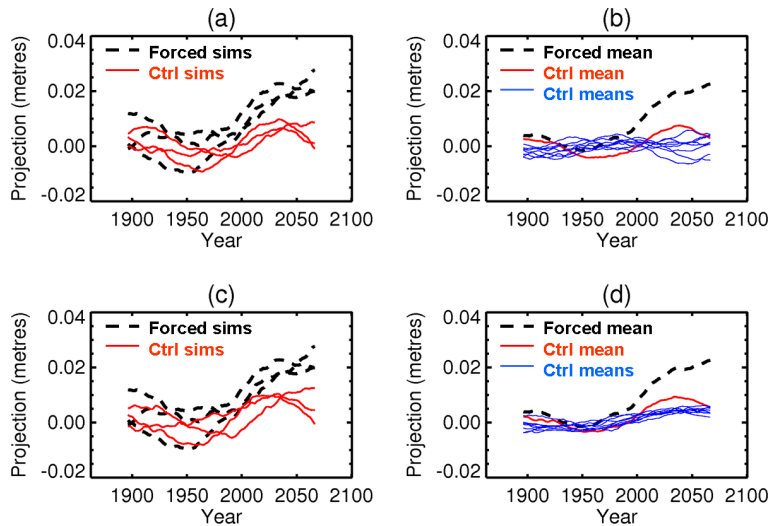


Fig. 6. Projection of each year's DSL anomaly field onto a pattern of change. **(a):** three individual HE forced simulations (broken black lines) projected onto the HE forced pattern of Fig. 5a and the three corresponding sections of control (red lines), projected onto the HE forced pattern of Fig. 5a. **(b)** Year-by-year average of the three HE forced simulations shown in **(a)** (broken black line) and year-by-year average of the three parallel sections of control shown in **(a)** (red line). Also shown are eight blue lines. Each of these shows a year-by-year average of a set of three sections of control with start years chosen at random, again projected onto the HE forced pattern of Fig. 5a. **(c)** Broken black lines exactly as in **(a)** and, for comparison, the three corresponding sections of control (red lines), this time projected onto the mean anomaly of the final hundred years of these three sections of control simulation (i.e. projected onto their "own" pattern). **(d)** Broken black lines exactly as in **(b)** and, for comparison, red line shows year-by-year average of the three sections of control shown in **(c)**. Also shown are eight blue lines. Each of these shows a year-by-year average of a set of three sections of control with start years chosen at random, again projected onto their "own" pattern. The point is that the forced signal (broken black line) is well outside the unforced noise (red and blue lines).

Dynamic sea level rise pattern from land-ice

T. Howard et al.

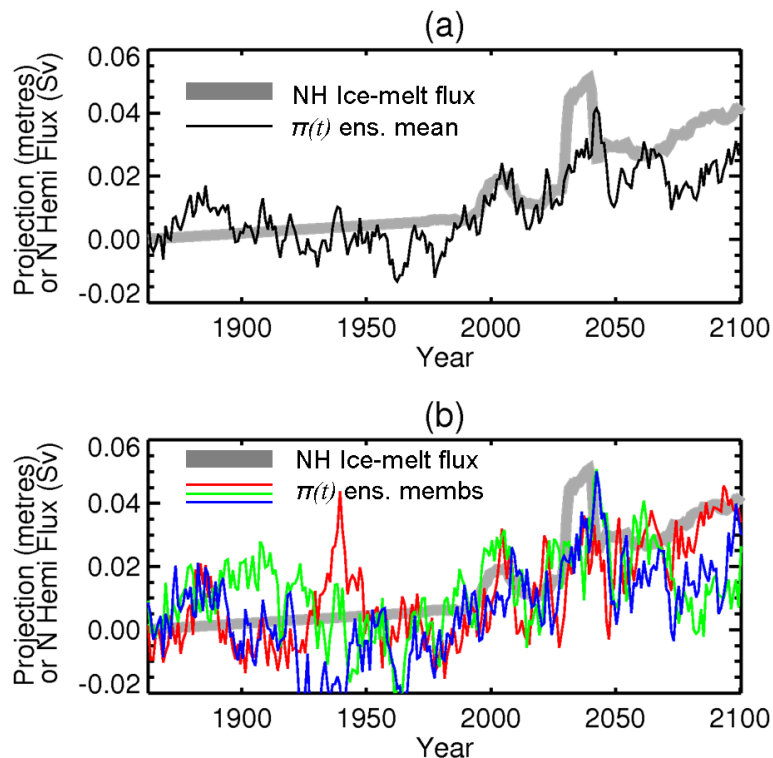


Fig. 7. Relationship between the northern-hemispherically-integrated ice-melt flux (thick grey line) for the HE scenario, and the year-by-year projection $\pi(t)$ (not smoothed) onto the North Atlantic DSL pattern which was identified as being associated with the ice-melt (Fig. 5a). **(a)** For the ensemble mean DSL anomaly (thin black line) **(b)** for DSL anomalies in each simulation (coloured lines).

**Dynamic sea level
rise pattern from
land-ice**

T. Howard et al.

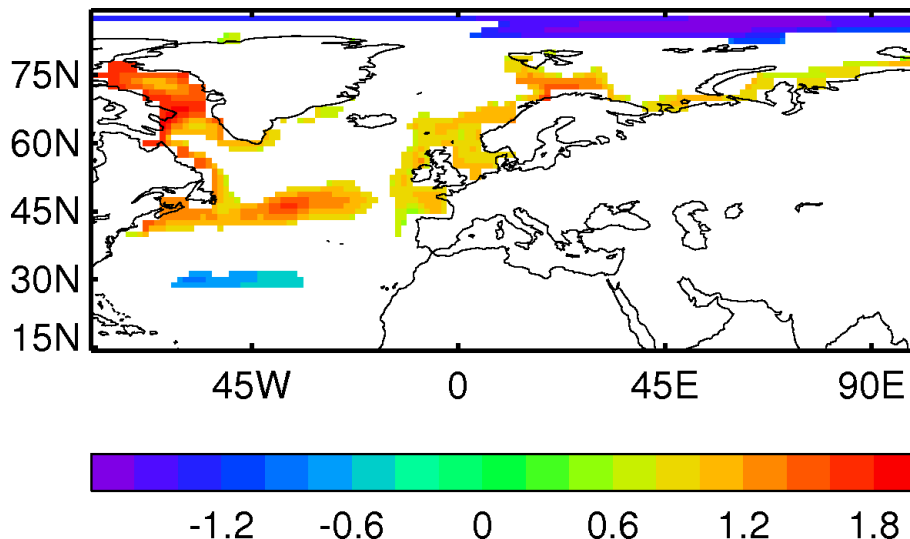


Fig. 8. Regression of ensemble-mean DSL against Northern Hemisphere-integrated ice melt flux (units of mSv^{-1}) for the HE ice scenario and region from 15° N to 90° N and 80° E to 100° W. Patterns are shown where more than 16% of the variance in DSL is explained by the fluxes (coefficient of determination is greater than 0.4): cut-off is chosen on the basis that no areas satisfy this condition in our unforced simulation; about 25% of the field area satisfies this condition for the HE ice scenario simulation.

Title Page

Abstract

Introduction

Conclusions

References

Tables

Figures

◀

▶

◀

▶

Back

Close

Full Screen / Esc

Printer-friendly Version

Interactive Discussion



**Dynamic sea level
rise pattern from
land-ice**

T. Howard et al.

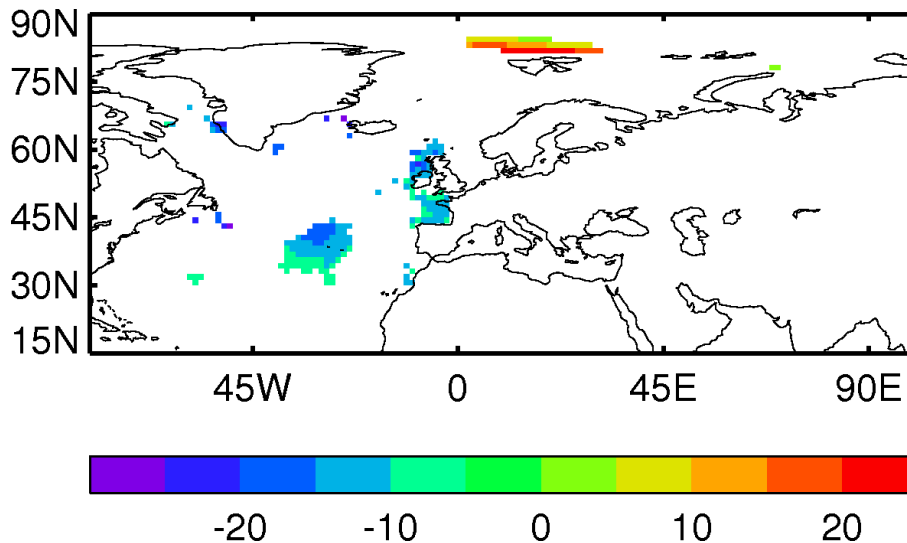


Fig. 9. As Fig. 8 but for ensemble-mean SST (units of $^{\circ}\text{C Sv}^{-1}$). Values are shown where the coefficient of determination is greater than 0.4, which covers approximately 9% of the sea area in our region of interest for our forced simulation. No such area arises in the control data.

[Title Page](#)[Abstract](#)[Introduction](#)[Conclusions](#)[References](#)[Tables](#)[Figures](#)[◀](#)[▶](#)[◀](#)[▶](#)[Back](#)[Close](#)[Full Screen / Esc](#)[Printer-friendly Version](#)[Interactive Discussion](#)

**Dynamic sea level
rise pattern from
land-ice**

T. Howard et al.

Title Page

Abstract

Introduction

Conclusions

References

Tables

Figures

◀

▶

◀

▶

Back

Close

Full Screen / Esc

Printer-friendly Version

Interactive Discussion

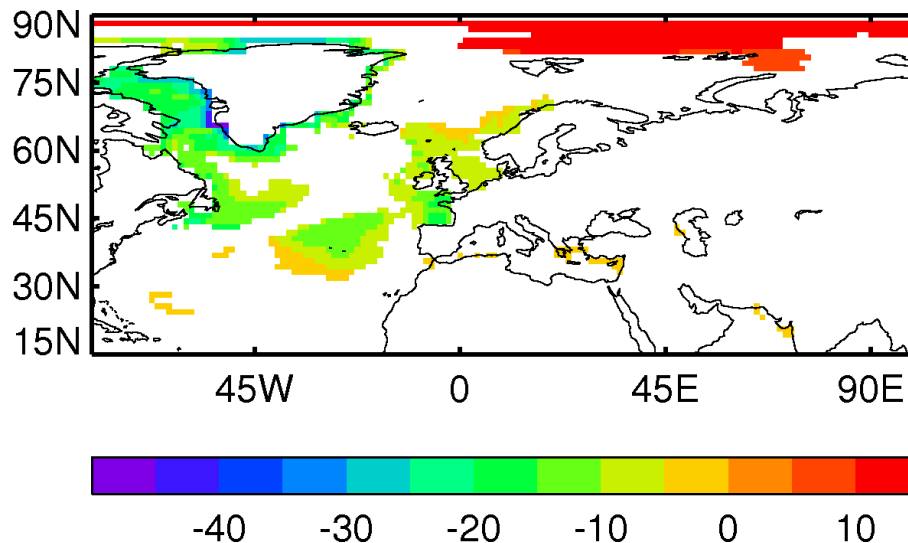


Fig. 10. As Fig. 8 but for ensemble-mean SSS (units of psu Sv^{-1}). Values are shown where the coefficient of determination is greater than 0.4, which covers approximately 25 % of the sea area in our region of interest for our forced simulation. The corresponding area is approximately 1 % in the control data.

Dynamic sea level rise pattern from land-ice

T. Howard et al.

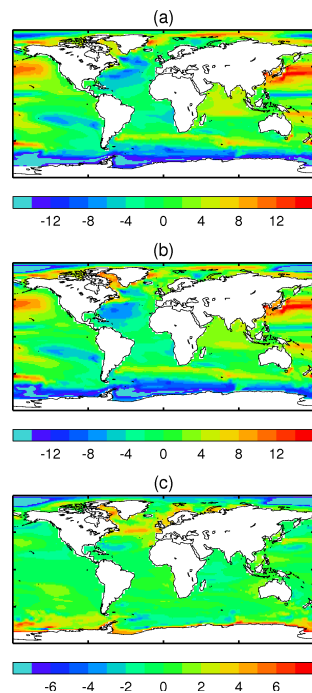


Fig. 11. DSL anomalies (cm) under the A1B greenhouse gas radiative forcing scenario **(a)** without the HE ice melt scenario (ice sheet freshwater fluxes around Greenland and Antarctic are from pre-industrial climatology), simulation A1B(s), **(b)** with the increasing HE fluxes, simulation A1B_HE(s) **(c)** the difference field giving the additional DSL change from the HE ice melt in the presence of A1B forcing. All fields are 100 yr averages for the period over 2000–2099. In contrast to the figures shown in Sect. 4.1, we have not assessed the statistical significance of the anomalies shown in **(c)**, because we do not have multiple realisations of the A1B simulation to compare against. The point here is that the pattern in panel **(c)** of this figure is very similar to the pattern of Fig. 3a.

[Title Page](#)
[Abstract](#)
[Introduction](#)
[Conclusions](#)
[References](#)
[Tables](#)
[Figures](#)
[◀](#)
[▶](#)
[◀](#)
[▶](#)
[Back](#)
[Close](#)
[Full Screen / Esc](#)
[Printer-friendly Version](#)
[Interactive Discussion](#)


Dynamic sea level rise pattern from land-ice

T. Howard et al.

Title Page

Abstract

Introduction

Conclusions

References

Tables

Figures

◀

▶

◀

▶

Back

Close

Full Screen / Esc

Printer-friendly Version

Interactive Discussion

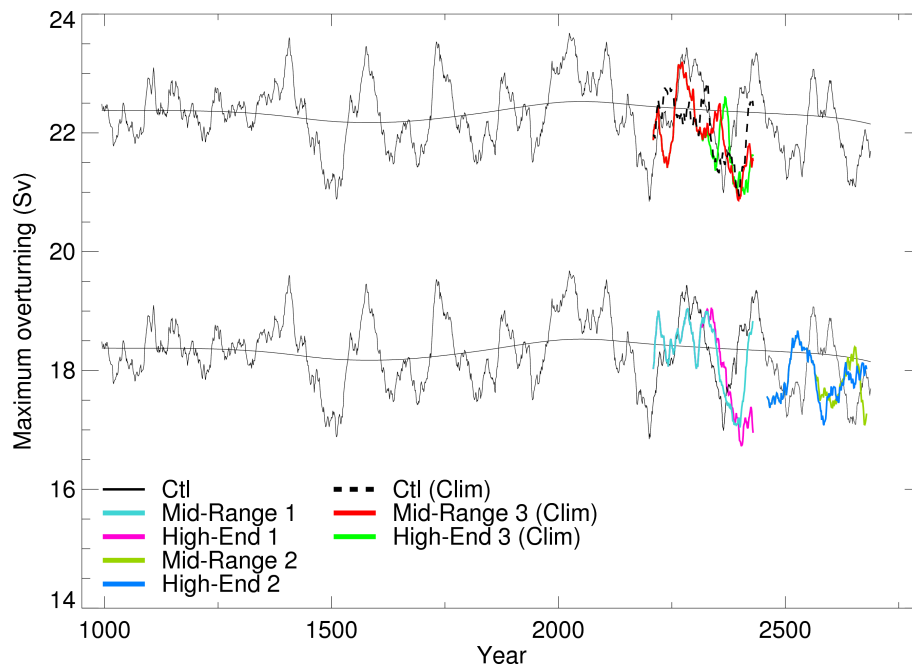


Fig. 12. MOC strength (maximum in the latitude range 30° N to 55° N, with running means of 21 yr applied) over pre-industrial control simulation (standard HadCM3 control and extension) and the concurrent HE and MR ice-melt scenarios simulations. Simulations marked “Clim” are those where the baseline runoff from the ice sheets is a monthly pre-industrial climatology (see Sect. 2.2). For clarity some of the simulations are shown shifted (by +4 Sv) against a similarly shifted copy of the control; these are the ones that appear above 20.5 Sv on the plot. Low frequency “drift” (cut-off of 600 yr) is shown by the thin black line.

Dynamic sea level rise pattern from land-ice

T. Howard et al.

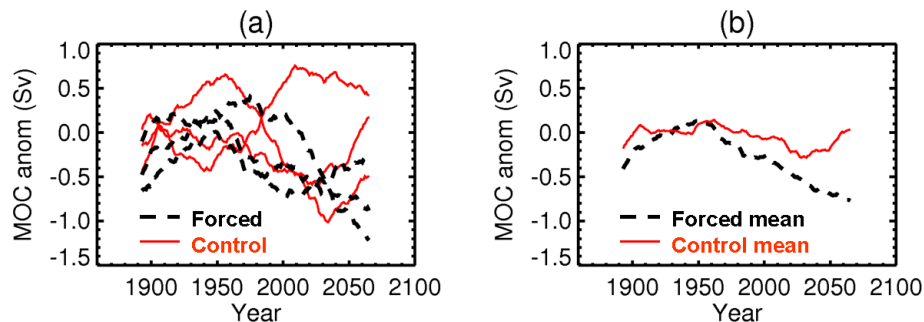


Fig. 13. MOC changes under the HE ice-melt scenario simulations. **(a)**: for each of the three HE ice-melt simulations (dashed black lines) along with the three concurrent sections of control simulation (solid red lines), **(b)**: average of the three HE simulations and control simulation sections shown in **(a)**. All smoothed with 69 yr running means.

Title Page

Abstract

Introduction

Conclusions

References

Tables

Figures

◀

▶

◀

▶

Back

Close

Full Screen / Esc

Printer-friendly Version

Interactive Discussion



**Dynamic sea level
rise pattern from
land-ice**

T. Howard et al.

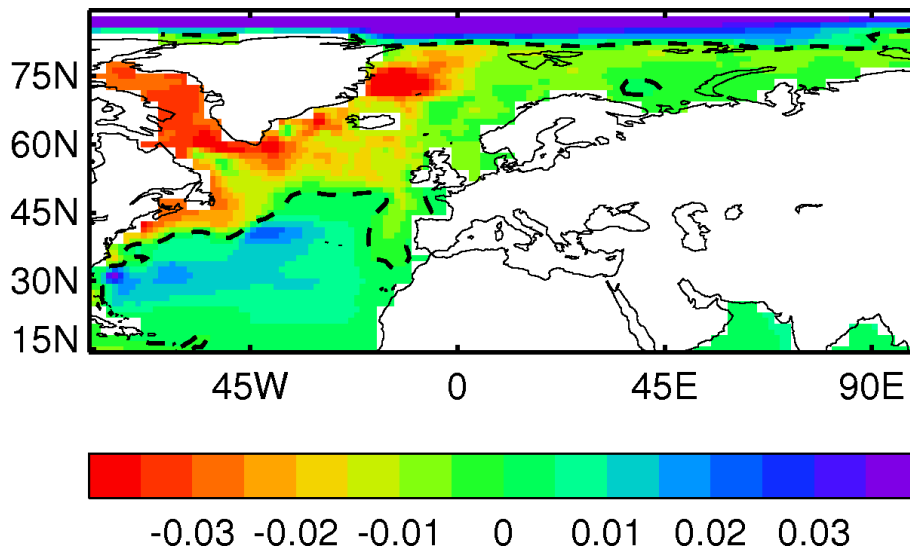


Fig. 14. Regression (mSv^{-1}) of low frequency variations (69 yr running means) in DSL anomaly against MOC, from the HadCM3 control simulation (1715 yr). Dashed line shows the zero contour. Drift first removed (see Sect. 2).

Title Page

Abstract

Introduction

Conclusions

References

Tables

Figures

◀

▶

◀

▶

Back

Close

Full Screen / Esc

Printer-friendly Version

Interactive Discussion

